

TA7

CG

CER 68/69-44b

COPY 2



Final Report
on
WIND TUNNEL INVESTIGATION OF SHAPES
FOR BALLOON SHELTERS

prepared by

Robert N. Meroney
Associate Professor
Civil Engineering Department

Erich J. Plate
Professor
Institut Wasser Bau III
Universitat Karlsruhe, Germany

Craig R. Symes
Graduate Research Assistant
Civil Engineering Department
Colorado State University

ENGINEERING RESEARCH

AUG 18 1970

PORTLANDS RESTING ROOM

for
National Center for Atmospheric Research

July, 1970

CER68-69RNM-EJP-CRS44b

MAILED FILE COPY

Final Report

on

WIND TUNNEL INVESTIGATION OF SHAPES
FOR BALLOON SHELTERS

prepared by

Robert N. Meroney
Associate Professor
Civil Engineering Department
Colorado State University

Erich J. Plate
Professor
Institut Wasser Bau III
Universitat Karlsruhe, Germany

Craig R. Symes
Graduate Research Assistant
Civil Engineering Department
Colorado State University

for

National Center for Atmospheric Research



July 1970

CER68-69RNM-EJP-CRS44b

ABSTRACT

In support of a balloon shelter development program at NCAR a series of wind tunnel tests were performed at the Fluid Dynamics and Diffusion Laboratory, Colorado State University. The study concerned the scaling criteria for such a simulation; velocity, turbulence, and frequency spectra downwind of four basic shelter shapes; the effect of screen material on shelter efficiency; and the influence of a simulated balloon presence upon the effectiveness of the shelter.

INDEX

1.0 Introduction 1

2.0 General Considerations of Similarity and Wind
Break Dynamics 3

2.1 The drag coefficient C_D for solid
shelters 3

2.2 The drag coefficient C_D for porous
shelters 5

2.3 The effect of h/δ 7

2.4 Pulsating forces on the balloon 7

3.0 Description of Experiments 8

3.1 Visualization 8

3.2 Velocity distributions 10

3.3 Turbulence intensity 11

3.4 Turbulence spectra 11

3.5 Pressure drop coefficients 12

4.0 Results and Discussion 13

4.1 Visualization 13

4.2 Velocity profiles 13

4.3 Turbulence intensity 14

4.4 Spectral analysis 14

4.5 Quantitative effect of included angle,
screen material and balloon presence 15

5.0 Conclusions 17

REFERENCES 19

TABLES

FIGURES

WIND TUNNEL INVESTIGATION OF SHAPES
FOR BALLOON SHELTERS

1.0 Introduction

A wind tunnel investigation was performed in the facilities of the Fluid Dynamic and Diffusion Laboratory, Colorado State University, on possible shelters for meteorological balloons. The purpose of the effort was to aid in the design of a screen which would reduce the wind to below 8 knots over a volume sufficient to assist with inflation and launching of balloons. The emphasis of the wind tunnel study was to determine the effects of basic shelter configurations and screen materials upon the sheltered area.

The wind tunnel program was organized to examine the following aspects of the shelter dynamics:

- A. Height, length, and breadth of the sheltered areas for various shelter configurations.
- B. Comparative effectiveness of a solid shelter compared with porous screen materials.
- C. Quantitative measurement of the frequency and intensity of gusts shed from the upper edge and sides of the proposed shelter configurations.
- D. Examination of low velocity areas at the sides of the shelter for short distances downstream of the shelter.

- E. Detailed study of the effect of two pieces of bug-screen material in the shelter frame, set at 45° to each other.
- F. The effect of changes in the included angle on sheltered area and gusting, and,
- G. The effect of the presence of a balloon shape within the sheltered area upon the effectiveness of the shelter.

Four basic shapes were tested, one consisted of a square plate set perpendicular to the wind, and the other three were of a wedge-type of same height and projection on the plane normal to the flow with apex angles of 90, 120, and 150 degrees. The models consisted of steel frames over which the screen materials had been sheltered, as shown in Fig. 1c. They were designed into sharp outer edges, so that separation would always occur at the edges. Two different screen materials were tested: ordinary fiberglass bug screen (.010" wire, 18 mesh) and a special dense mesh fiberglass material provided by NCAR (~.15 open area).

The presence of a partially inflated balloon was simulated by a rigid "ice-cream" shaped wooden model. The model was $3/4$ inch diameter at the base and tapered to a 4 inch diameter hemispherical cap. The model was of course not compliant to gust effects and stood a total of 10 inches high.

2.0 General Considerations of Similarity and Fluid Dynamics of Wind Breaks

In some earlier work (Plate and Lin (1965) "The velocity field downstream from a two-dimensional model hill") it is shown that modeling of a field situation in a laboratory is accomplished if C_D (i.e., the drag coefficient of the shelter) and the ratio h/δ are the same in both field and laboratory, where the length h is the structure height and δ is the thickness of the boundary layer. Although these requirements were for two-dimensional flow fields, it can be expected that only minor modification would be required for the three-dimensional counterpart.

2.1 The drag coefficient C_D for solid shelters

Constant drag coefficients C_D can be obtained approximately by having sharp edges of the shelters both in model and prototype. Then the drag coefficient defined by

$$C_D = \frac{D}{\frac{1}{2} \rho u_\infty^2 h \cdot w} \quad (1)$$

where D is the drag on the shelter, becomes independent of the Reynolds number $u_\infty h/\nu$. In this equation, h is the height and w the breadth of the projection of the shelter on a plane perpendicular to the direction of the ambient air flow u_∞ (at some reference height). Ordinarily C_D would be a function of Reynolds number. However, by sharpening the edges of the shelter, the separation line of the boundary layer on the shelter becomes fixed, resulting in a

C_D which is independent of the Reynolds number. It does, however, depend slightly on h/δ , but this dependency is not critical and can be taken care of by making the boundary layer of the approach flow as thick as possible.

The drag coefficient not only determines the drag on the shelter but also the shape of the flow field downstream from the shelter. In general, the larger C_D , the larger will be the sheltered area, but evidently at the price of a larger drag force, as well as higher turbulence levels.

For a solid screen, or a square flat plate, it is possible to obtain the drag coefficient, to a first approximation, from the relation:

$$\frac{C_D \text{ infinite plate}}{C_D \text{ rectangular plate}} \left| \begin{array}{l} \text{in free stream} \\ \text{in boundary layer} \end{array} \right. \quad (2)$$

or (see Rouse (1950), p. 126, for free stream ratio)

$$\frac{1.90}{1.16} = \frac{0.8}{C_D} \quad (3)$$

when the value of 0.8 for the drag coefficient of the infinite plate in a boundary layer has been taken from experimental results of Plate (1964). Consequently:

$$C_D = \frac{1.16}{1.90} \cdot 0.8 = 0.5 \quad (4)$$

to a first approximation.

Some measurements of Vichery (1968) for a plate which was neither fully in the free stream nor on a floor were

found to yield $C_D = 1.0$, approximately, which falls between the assumed free stream value of 1.16 and the calculated boundary layer value of 0.5. A safe value, to be used in calculation, might therefore be taken as about $C_D = 0.7$.

In the quoted paper, Vichery also points out that in addition to the mean drag, there also occurs a fluctuating drag whose RMS - value might be as much as 10% of the mean. He does not give a peak value, but a suitable safety factor should be used. In view of the fact that the structure of the shelter will be very light, a safety factor of at least two is recommended, i.e., for the design of the structure, $C_D = 1.0 - 1.2$ should be used.

2.2 The drag coefficient C_D for porous shelters

It is very likely that the effect of porosity is also a Reynolds number effect, but this time the Reynolds number should be based on the properties of the screen material. Since air flow and viscosity in model and prototype are the same, it is required that the screens are the same also, to meet Reynolds number similarity. Actually, however, it is found that for a given screen material the aerodynamic behavior is practically independent of Reynolds number. A measure of the aerodynamic behavior can be obtained by determining the pressure drop Δp across a screen which passes a velocity of \bar{u} fps. The pressure drop coefficient

$$c_p = \frac{\Delta p}{\frac{1}{2} \rho \bar{u}^2} \quad (5)$$

should become independent of the Reynolds number.

For a porous screen, the pressure drop coefficient yields a measure of the force exerted on the screen. Let \bar{u} be the velocity observed, in the model case directly downstream of the screen. Then, to a rough approximation:

$$D = c_p \frac{1}{2} \rho \bar{u}^2 \cdot w \cdot h \quad (6)$$

or, if the reduction factor c is introduced:

$$c = \frac{\bar{u}}{u_\infty} \quad (7)$$

which signifies the reduction of velocity obtained by a screen, then:

$$D = c_p c^2 \cdot \frac{1}{2} \rho u_\infty^2 w \cdot h \quad (8)$$

For a given screen material and shelter shape, the coefficients c_p and c are found from wind tunnel experiments.

Comparison of Eqs. 1 and 8 shows that for a porous screen we have:

$$C_D = c_p c^2 \quad (9)$$

The experiments show that for a porous screen, both c and c_p are approximately independent of velocity, so that C_D is found independent of Reynolds number for porous screens also--provided that the screens are the same in model and prototype.

For the bug screen material used, we find a value of $c_p = 0.62$ and a reduction factor $c = 0.5$. Consequently, the equivalent drag coefficient, according to Eq. 9 is

$$C_D = 0.62 \cdot \frac{1}{4} = 0.16 \quad .$$

It goes without saying that the relation EQ. 9 is valid only for $C_D < 0.5 \div 0.7$. Once $C_D = 0.5 \div 0.7$ is reached, a screen behaves like a solid screen regardless of its actual porosity.

2.3 The effect of h/δ

The parameter h/δ determines mainly the velocity distribution downstream of the shelter, outside the sheltered region. For the sheltered region its effect is mainly on the drag coefficient. C_D varies, for thick boundary layers, approximately proportional to $(h/\delta)^{2/7}$ in the case of an infinitely wide shelter. For a finite width shelter, the effect should be even smaller, and thus, if we just make the profile approaching the shelter roughly logarithmic and as thick as possible, the values of C_D obtained in the experiments should be transferable without much error to the atmospheric conditions, which leads to the proposed value of $C_D = 0.5 \div 0.7$.

2.4 Pulsating forces on the balloon

A sharp edged device like the balloon shelter model is very likely to shed regular eddies, (of Karman type vortices) which will be the dominant feature in the large scale turbulence. Unfortunately, for the experimental results of this preliminary study, no satisfactory measurements of the eddy shedding velocities were obtained. It can, however, be expected that the frequency f of the dominant eddies is given approximately by the Strouhal frequency obtained from the relation

$$St = \frac{fW}{u_{\infty}} = 0.08 \text{ to } 0.11$$

where St is Strouhal number, which according to results of Vichery (1968) is approximately constant and lies within the indicated range, and f is the peak frequency.

Typically, for a shelter of 70 ft. width, one would expect a dominant frequency of about (at 30 ft/sec)

$$f = \frac{u_{\infty}}{W} St = \frac{30}{70}(0.1) \approx 0.45 \text{ Hz} .$$

For the one foot wide model examined in the wind tunnel, a similar calculation would suggest a dominant frequency of about (at 30 ft/sec)

$$f = \frac{30}{1}(0.1) \approx 3 \text{ Hz} .$$

Unfortunately this value is at the lower range of reliability for wind tunnel instrumentation and may not be apparent readily. More accurate results should be obtained in the testing program for the final design or in a field program.

3.0 Description of Experiments

3.1 Visualization

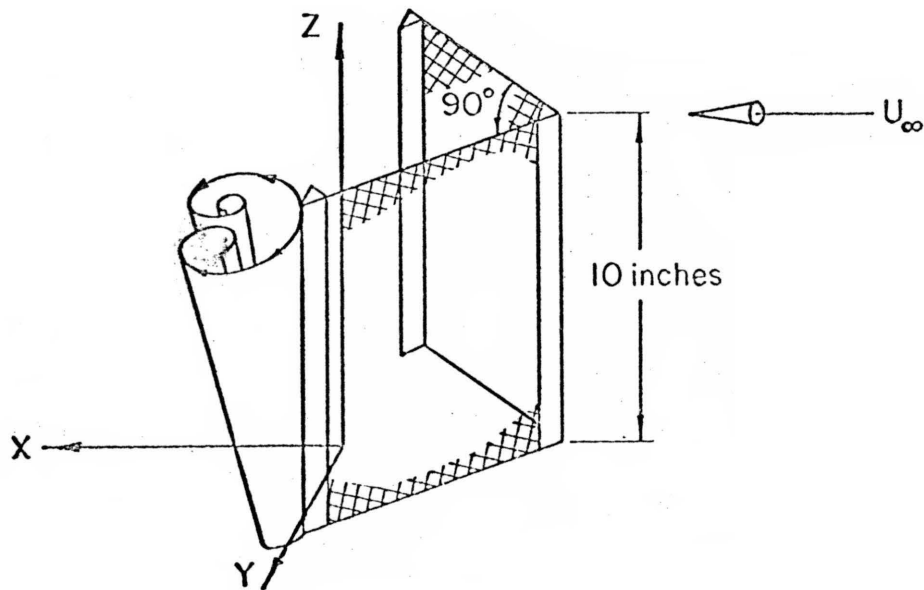
For this series of experiments three different shelter angles were tested; 90 degrees, 120 degrees and 150 degrees included angle. Tests on the three shelters were performed with one piece of bug-screen held in the frame. A further test was carried out on the 120 degree shelter using two

pieces of bug-screen held in the frame, set at 45 degrees to each other.

To obtain an estimate of the amount of flow deflected along a single upstream face of the 90° shelter smoke tracers were released upstream of the shelter. For very low free-stream velocities the majority of the smoke was deflected right along the upstream face (see photograph 1). For higher freestream velocities the smoke passed through the screen about halfway along the screen surface (see photograph 2). With the balloon model placed behind the screen the smoke pattern was not observably changed.

The other visualization technique involved looking at the motion of a small cork ball which was attached by thread to a long wire rod. Holding the wire rod from outside the flow field, the ball could be located at positions about the shelter. The areas of main interest were the shelter sides and top edges. No rotation of the ball was observed over the top edges, however at the side edges as the ball was drawn across a vertical side support (in the direction of decreasing Y), the rapid rotation of the ball changed direction abruptly. A short distance inside the support (that is, in the sheltered region) the ball rotation slowed and ceased.

It is felt that this vortex phenomena at the shelter edges is due entirely to the vertical supports. The direction of the outer vortex follows that percentage of flow deflected along the screen and the freestream flow as it sweeps around



the trailing edges, while the opposing direction of rotation of the inner vortex is due to the flow passed through the screen near to the support.

3.2 Velocity distributions

Vertical distributions of horizontal mean velocities were taken to map out the sheltered region. Using a coordinate system where X is the distance downstream measured from the shelter trailing edge, Y is the transverse co-ordinate measured from the screen center line and Z is in the vertical direction, velocity measurements were taken for $X = 0(3)18$, $Y = 0(3)12$ and $Z = 0(5)15$ inches, (only one side of the shelter need be considered in view of the symmetry of the shelter about the XZ plane.)

Velocities were obtained using a pitot-static tube with a Transonic pressure transducer. A freestream velocity range of 20 feet per second to 50 feet per second was used on the

4 different shelters. The results of these measurements appear in Table 1.

3.3 Turbulence intensity

A gross measure of the tendency of the balloon shelter to dissipate the kinetic energy of the unrestrained wind is the turbulence intensity $\overline{u'^2}$ when u' is the fluctuating velocity component (with time mean zero) in the direction of the mean local flow velocity. The overbar denotes the time mean. Due to the limitations of the RMS-Analyzers utilized, these data are of frequencies higher than 2 cps, they are thus not representative of the low frequency end of the spectrum, which is of greatest importance for balloon sheltering. It also became clear that one area of major interest was the side edges of a shelter. Further examination of this area involved measuring turbulence intensities and taking frequency analyses of the eddy shedding at the edges. Turbulence intensities were measured using a Disa constant temperature anemometer, type 55A01.

3.4 Turbulence spectra

We took two types of turbulence data: pressure fluctuations of a pitot-static tube recordings at a distance of 3" from the centerline at four different downstream distances of the NCAR screen square plate and wedge, at one height of 6" (= 1/2 h) above the floor. These data, recorded on strip charting give an indication of the low frequency turbulence which is likely to effect the balloons. However,

we cannot detect any low frequency component in the recordings which might be significant. We feel that this result is due to the fact that eddy shedding will be most pronounced at the edges of the screens, where measurements were not taken.

A second set of turbulence data was obtained from the output signal of a constant temperature hot wire anemometer. Special attention was given to the shear flow at the shelter edge.

The signal from the anemometer was displayed on an oscilloscope and analyzed using General Radio's Graphic Level Recorder type 1510-A, coupled to a Sound and Vibration Analyzer, type 1911-A. (See Fig. 2a). This equipment claims a frequency response from 2.5 to 25 k Hz

3.5 Pressure drop coefficients

Pressure drop coefficients c_p were obtained by stretching screens across the whole cross section of the wind tunnel and measuring velocity and pressure drop across the screen with two pitot-static tubes located one upstream and one downstream of the screen. For the NCAR screen we found a pressure drop coefficient c_p of 22--implying an almost solid screen--independent of Re number. For the bug screen, the pressure drop coefficient was found to be 0.62. For bug screen prepared in a double layer with a 45° angle between the mesh orientation the pressure drop coefficient was about 1.25. Again, all Reynolds number dependencies, if

existing, were hidden in the scatter of the experimental results.

4.0 Results and Discussion

4.1 Visualization

From the techniques described it appears that all shelter angles give approximately the same sheltered region with a velocity reduction of about 50 percent. Eddy shedding is an important feature but is confined to the side edges of the shelter and does not affect the sheltered area. No other large scale vortices related to the shelter geometry were observed.

With the wooden balloon model in place a marked decrease in velocity on the centerline with an increase around the sides and over the top of the balloon was observed. A short distance downstream these two effects seemed to combine to produce a flow pattern similar to that of the "no balloon" case.

4.2 Velocity profiles

The profiles of the approach velocity for the shelters are shown in Fig. 2. From the profiles, isotachs were constructed which are shown in Figs. 3 to 13. Two types of figures are shown. Profiles along the centerline, to show the reduction of wind velocity in a plane along the center at different velocities, are given in Figs. 3, 5, 6, 8, 9-3, 11, and 12-3. Note that downwind distances from the wedge

are measured from the downwind edges of the model. The remainder of the isotach figures show cross sections through the sheltered regions. Only half of the sheltered region is shown, since the (vertical) z-axis is an axis of symmetry.

4.3 Turbulence intensity

Using the Disa hot-wire anemometer the turbulence intensity distribution around the shelters was investigated. The freestream turbulence level was about 3 percent. Behind the screen section of a shelter the turbulence level was very low (4 percent), but on the centerline (i.e., behind the center support) the level rose to 20 percent. The effect was most marked at the edges, 40 percent intensity being the general value. These high values at the edges are consistent with the vortex ball investigation. The vortex ball, however, failed to indicate the relatively high turbulence level due to the center support. Profiles of $\overline{u'^2}$ along a distance $1/4w$ off the centerline are shown in Fig. 14. Table 2 summarizes measurements available.

4.4 Spectral analysis

The signal from the anemometer was subjected to a frequency spectrum analysis, the eddy shedding frequency at the edges being the major area of interest. The expected frequency of the dominant eddies, given approximately by the Strouhal frequency, was of the order 10 Hz. Extensive investigation failed to isolate this frequency. It is felt

that the low frequency limit of the equipment may be responsible for this deficiency. Another possibility is that for porous structures the realm of regular frequencies ceases for $Re > 10^5$. Even for cylinders measurements for high Re numbers are very sparse. Roshko has suggested a Strouhal gap exists between 10^5 and 10^7 for eddy shedding from cylinders (Markovin, (1964)). Although the Re number for the prototype shelter size may well be greater than 10^7 , one may have difficulty in identifying a specific maximum shedding frequency since 1) the maximum becomes increasingly blurred at high Re number, and 2) the flow through the porous screen may never allow significant lateral pressure excursions to occur such that an alternating structure may be observable.

At this time, it is therefore only possible to use the quoted results by Vichery as a rough guide, and to prepare a more extensive record of the turbulence, at the edges of the screen, during tests on a field model.

4.5 Quantitative effect of included angle, screen material and balloon presence

The velocity reduction behind the shelters for the different configurations appear in Table 1. For the single screen shelter the velocity reduction for all angles was over 50 percent. For the double screen shelter the reduction was about 75 percent with pressure coefficient increasing to twice that of the single screen case.

Two dimensionless parameters, ξ , a mass flux parameter and ψ , a momentum flux parameter were defined,

$$\xi = \frac{\int_0^y \rho u \, dy}{\rho U_\infty L}$$

and

$$\psi = \frac{\int_0^y \rho u (U_\infty - u) \, dy}{\rho U_\infty^2 L} .$$

u is the velocity behind the shelter (i.e., those velocities in Table 1), U_∞ is the freestream velocity and L is the total width of the shelter ($L = 12$ inches). These parameters were calculated for the wake of the different shelters and are tabulated in Tables 3 and 4. It can be seen that there is little variation in the parameters over the set of single screen shelters suggesting that shelter shape has little effect on the downstream region. In the double screen case, the decrease in these parameters is consistent with our intuition. Again little variation is seen over the range of freestream velocities.

The momentum flux parameter ψ may be viewed as a pseudo-drag coefficient in the sense that it is a measure of the blocking effect of the shelter. It is, of course, not exactly a drag coefficient, since the fluid motion is three dimensional and corrections must be made for static pressure variations when the transverse is close to the shelter. Schlichting (1968) discusses correction methods to be applied to drag calculations from measurements in the mean wake vicinity.

5.0 Conclusions

On the basis of the reported experiments, the following conclusions on the design of a balloon shelter are drawn.

1. Porous shelter surfaces, as compared to solid (or almost solid surfaces) have a considerably lower turbulence level associated with them, but a mean velocity level which is higher in the sheltered region. Furthermore, the forces on a porous screen are much smaller. A rough estimate gave drag coefficients for the square plate data of 0.5 to 0.7 and 0.16 for solid and bug screen surfaces respectively.
2. The shelter angle has no noticeable effect on velocity reduction, turbulence level or flow pattern.
3. Velocity reduction for all angles with single screen is over 50 percent with 75 percent reduction in the double screen case. The pressure coefficient is doubled for the double screen case. Neither the flow pattern nor the percentage reductions attained depended on the ambient velocity U_{∞} . Consequently, it is felt that prototype screen and model screens should be the same. It is recommended that a material should be used for the screens which is slightly denser than the bug screen, such as a double layer of bug screen or equivalent.

4. The balloon presence produces higher velocities around the balloon surface. Downstream the flow pattern returns to the "no balloon" case.
5. Eddy shedding from the structure's edges could interact with the balloon if the shelter was too narrow.
6. A blockage near the structure may occur due to the vertical side supports. The velocity decrease behind these supports recovers quickly with distance downstream.
7. A square plate shelter provides a larger sheltered area, but a more intense turbulence intensity than a wedge shaped design. On this basis, and on the basis of construction convenience, it is recommended that the wedge be used, in a suitable modification to meet structural requirements.
8. Finally, it is recommended that on the basis of these findings the desired shelter should be engineered to fit suitably into the sheltered areas indicated in Figs. 3 to 13.

REFERENCES

- Markovin, M. V. (1964), "Flow around circular cylinder - A kaleidoscope of challenging fluid phenomena," Proc. of Symposium on Fully Separated Flows, ASME, May 18-20, 1964; pp 102-118.
- Plate, E. (1964), "The drag on a smooth flat plate with a fence immersed in its turbulent boundary layer," ASME paper No. 64 FE-17.
- Plate, E. and C. Y. Lin (1965), "The velocity field downstream from a two-dimensional model hill." Final Report, Part I, U. S. Army Materiel Agency, Contract DA-AMC-36-039-63-G7.
- Rouse, H. (1950), editor, "Engineering Hydraulics." J. Wiley, New York.
- Schlichting, H. (1968), "Boundary layer theory." McGraw Hill Book Company, New York.
- Vichery, B. J. (1968), "Load fluctuations in turbulent flow." Proc. ASCE, Journal Engr. Mech. Division, Vol. 94, paper No. EMI.

TABLE 1

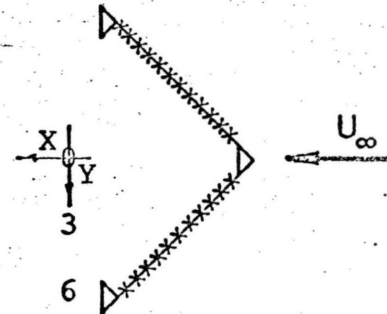
VELOCITY PROFILES (FEET/SECOND)

X, Y, Z Co-ordinates in Inches

90 Degree Shelter (No Balloon) $U_{\infty} = 19.0$ Ft./Sec.

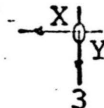
Z = 5 Inches

	15	12	9	6	3	
	6.83	5.94	-	7.04	7.24	
	9.04	8.01	-	9.66	9.66	
	10.10	8.37	-	8.01	2.41	
	16.20	15.27	-	16.20	15.74	



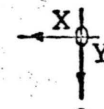
Z = 10 Inches

	15	12	9	6	3	
	10.80	9.04	-	7.04	7.04	
	9.35	9.35	-	9.66	10.10	
	10.80	10.10	-	10.10	4.52	
	17.91	18.71	-	17.91	17.91	

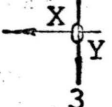
 $U_{\infty} = 31.5$ Ft./Sec.

Z = 5 Inches

	15	12	9	6	3	
	11.46	11.46	-	12.19	13.23	
	15.74	16.20	-	17.08	18.71	
	17.08	16.20	-	13.77	8.71	
	27.53	27.00	-	28.06	28.08	

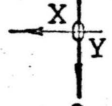


z = 10 Inches

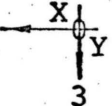
15	12	9	6	3	
19.47	18.71	-	13.23	12.55	
17.08	17.08	-	17.91	3	
18.71	19.47	-	17.91	6	
31.02	30.55	-	29.58	9	

U_∞ = 48.6 Ft./Sec.

z = 5 Inches

15	12	9	6	3	
17.08	17.08	-	18.71	18.71	
24.15	24.15	-	25.90	3	
24.75	24.15	-	20.91	6	
40.41	39.68	-	40.77	9	

z = 10 Inches

15	12	9	6	3	
28.06	25.33	-	19.47	17.91	
25.33	25.33	-	26.45	3	
27.53	27.53	-	28.06	6	
43.20	42.52	-	43.20	9	

90 Degree Shelter (with Balloon)

$$\underline{U_{\infty} = 19.0 \text{ Ft./Sec.}}$$

 $Z = 5 \text{ Inches}$

15	12	9	6	3		
-	-	2.41	3.82	2.53		
6.39	-	6.16	7.04	12.07		3
9.04	-	8.87	8.87	7.64		6
-	-	16.64	16.73	16.64		9

 $Z = 10 \text{ Inches}$

15	12	9	6	3		
-	-	10.25	9.81	10.25		
10.10	-	10.66	11.33	12.07		3
9.96	-	10.25	10.25	10.10		6
-	-	18.31	18.47	18.55		9

120 Degree Shelter (No Balloon)

$U_{\infty} = 19.0 \text{ Ft./Sec.}$

z = 5 Inches

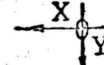
12	9	6	3	
5.66	5.92	6.39	7.24	
8.01	8.37	8.71	9.96	
8.17	8.37	7.83	3.82	
16.11	16.02	16.20	16.38	

z = 10 Inches

12	9	6	3	
6.39	6.39	6.61	6.61	
8.54	8.87	9.35	9.96	
8.54	8.19	7.44	3.82	
16.90	17.50	17.50	18.15	

120 Degree Double Screen Shelter (No Balloon) $U_{\infty} = 19.0$ Ft./Sec. $z = 5$ Inches

12	9	6	3
3.82	4.00	4.52	5.40
4.83	5.26	5.79	6.61
4.97	5.12	5.53	2.96
13.77	14.79	16.20	16.64



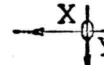
3

6

9

 $z = 10$ Inches

12	9	6	3
3.82	4.18	4.83	6.27
4.83	4.83	5.12	5.66
5.26	5.26	5.26	2.41
15.74	17.08	17.66	17.50



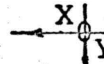
3

6

9

 $U_{\infty} = 31.5$ Ft./Sec. $z = 5$ Inches

12	9	6	3
5.40	5.92	6.83	8.87
8.37	9.35	10.10	11.20
8.87	9.20	9.20	5.4
24.75	26.45	27.53	27.00



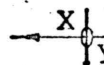
3

6

9

 $z = 10$ Inches

12	9	6	3
5.92	6.61	8.01	9.81
8.20	8.87	9.81	11.33
9.35	9.35	9.35	3.19
25.90	26.45	29.08	29.08



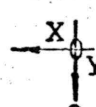
3

6

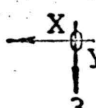
9

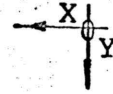
$$U_{\infty} = 48.6 \text{ Ft./Sec.}$$

$$z = 5 \text{ Inches}$$

	12	9	6	3		
	6.61	8.01	9.35	11.33		
	11.83	13.77	15.27	17.08		3
	13.12	13.77	13.77	14.08		6
	36.62	37.41	39.68	39.68		9

$$z = 10 \text{ Inches}$$

	12	9	6	3		
	8.54	9.20	10.80	13.23		
	12.55	14.29	14.69	17.50		3
	14.39	14.69	15.08	13.77		6
	40.77	40.05	42.86	42.86		9

150 Degree Shelter (No Balloon) $U_{\infty} = 19.0 \text{ Ft./Sec.}$ $z = 5 \text{ Inches}$ 

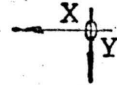
No Measurements taken

 $z = 10 \text{ Inches}$

15	12	9	6	3		
-	-	7.64	6.61	6.16		
7.83	8.19	8.37	8.71	8.87		3
9.35	-	8.37	7.44	5.40		6
-	-	18.31	18.31	18.23		9

150 Degree Shelter (With Balloon) $U_{\infty} = 19.0$ Ft./Sec. $z = 5$ Inches

No Measurements Taken

 $z = 10$ Inches

	12	9	6	3		
	8.54	8.87	10.39	-		
	9.35	10.10	11.20	-		3
	9.66	9.35	8.71	-		6
	19.02	19.09	19.09	-		9

TABLE 2

TURBULENCE INTENSITY (DIMENSIONLESS)

90 Degree Shelter (No Balloon)

 $U_{\infty} = 9.96$ Ft./Sec. $z = 5$ INCHES

12	9	6	3	x_0	y
			0.1387		
			0.0380		3
			0.4374		6
			0.0453		9

 $z = 10$ INCHES

12	9	6	3	x_0	y
			0.1904		
			0.0332		3
			0.4582		6
			0.0380		9

 $z = 15$ INCHES

	3	x_0	y
	0.0254		
	(For all Y)		

90 Degree Shelter (No Balloon) $U_{\infty} = 19.0$ Ft./Sec.

Z = 5 INCHES

12	9	6	3	X_{0Y}
0.1291	0.1460	0.1508	0.1497	
0.0619	0.0517	0.0446	0.0447	3
0.1538	0.1896	0.2701	0.4688	6
0.0722	0.0579	0.0525	0.047	9

Z = 10 INCHES

12	9	6	3	X_{0Y}
0.2649	0.2398	0.2011	0.1953	
0.0926	0.0659	0.0479	0.0386	3
0.1532	0.1799	0.2352	0.3756	6
0.0567	0.0451	0.0391	0.0379	9

Z = 15 INCHES

12	9	6	3	X_{0Y}
0.0303	0.0285	0.0285	0.0270	

(For all Y)

90 Degree Shelter (With Balloon) $U_{\infty} = 19.0$ Ft./Sec.

Z = 5 INCHES

15	12	9	6	3	X_{0Y}
-	-	0.5704	0.4300	0.4221	
0.3181	-	0.4029	0.3571	0.1247	3
0.1679	-	0.1673	0.2286	0.3893	6
-	-	0.0517	0.0478	0.0454	9

Z = 10 INCHES

15	12	9	6	3	X_{0Y}
-	-	0.3287	0.3295	0.3721	
0.1880	-	0.1661	0.1146	0.0464	3
0.1536	-	0.1750	0.2196	0.3304	6
-	-	0.0478	0.0401	0.0568	9

150 Degree Shelter (No Balloon) $U_{\infty} = 19.0 \text{ Ft./Sec.}$ $z = 5 \text{ INCHES}$ $x_0 y$

No measurements taken

 $z = 10 \text{ INCHES}$

15	12	9	6	3	$x_0 y$
-	-	0.2338	0.3214	0.3437	
0.1056	0.1002	0.0814	0.0714	0.0667	3
0.1504	-	0.2148	0.2721	0.3580	6
-	-	0.1107	0.0913	0.0410	9

150 Degree Shelter (With Balloon) $U_{\infty} = 19.0 \text{ Ft./Sec.}$

Z = 5 INCHES

No measurements taken

 $X_0 Y$

Z = 10 INCHES

15	12	9	6	3	
-	.2954	0.3108	0.3613	-	$X_0 Y$
-	0.1969	0.1910	0.1163	-	3
-	0.1468	0.1450	0.1880	-	6
-	0.0726	0.0517	0.0431	-	9

TABLE 3

MASS FLUX PARAMETER ξ (DIMENSIONLESS)

ξ is calculated for the various freestream velocities at $Z = 10$ and X coordinate shown below.

90 Degree Shelter (No Balloon)

	X = 3	X = 6	X = 12	X = 15
$U_{\infty} = 19.0$	0.48	0.57	0.58	0.61
$U_{\infty} = 31.5$	0.54	0.61	0.65	0.65
$U_{\infty} = 48.6$	0.52	0.59	0.59	0.61

90 Degree Shelter (With Balloon)

	X = 3	X = 6	X = 9
$U_{\infty} = 19.0$	0.64	0.63	0.62

120 Degree Shelter (No Balloon)

	X = 3	X = 6	X = 9	X = 12
$U_{\infty} = 19.0$	0.46	0.51	0.51	0.50

120 Degree Double Screen Shelter (No Balloon)

	X = 3	X = 6	X = 9	X = 12
$U_{\infty} = 19.0$	0.35	0.38	0.38	0.35
$U_{\infty} = 31.5$	0.36	0.40	0.37	0.35
$U_{\infty} = 48.6$	0.41	0.39	0.37	0.35

150 Degree Shelter (No Balloon)

	X = 3	X = 6	X = 9
$U_{\infty} = 19.0$	0.46	0.50	0.52

150 Degree Shelter (With Balloon)

	X = 6	X = 9	X = 12
$U_{\infty} = 19.0$	0.61	0.59	0.58

TABLE 4

MOMENTUM FLUX PARAMETER ψ (DIMENSIONLESS)

ψ calculated for the various freestream velocities at $Z = 10$ and X coordinate shown below.

90 Degree Shelter (No Balloon)

	X = 6	X = 12	X = 15
$U_{\infty} = 19.0$	0.21	0.21	0.22
$U_{\infty} = 31.5$		0.21	0.21
$U_{\infty} = 48.6$		0.23	0.22

90 Degree Shelter (With Balloon)

	X = 6	X = 9
$U_{\infty} = 19.0$	0.21	0.21

120 Degree Shelter (No Balloon)

	X = 12	X = 15
$U_{\infty} = 19.0$	0.21	0.22

120 Degree Double Screen Shelter (No Balloon)

	X = 12	X = 15
$U_{\infty} = 19.0$	0.17	0.18
$U_{\infty} = 31.5$	0.19	0.18
$U_{\infty} = 48.6$	0.19	0.18

150 Degree Shelter (No Balloon)

	X = 6	X = 9
$U_{\infty} = 19.0$	0.21	0.21

150 Degree Shelter (With Balloon)

	X = 6	X = 9	X = 12
$U_{\infty} = 19.0$	0.20	0.21	0.21

PHOTO 1

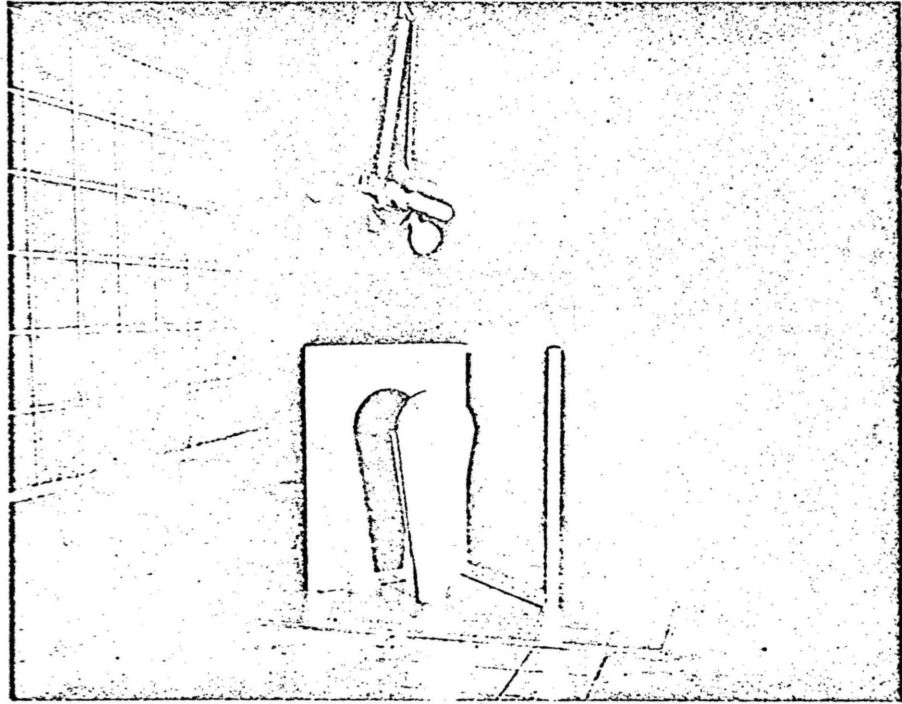
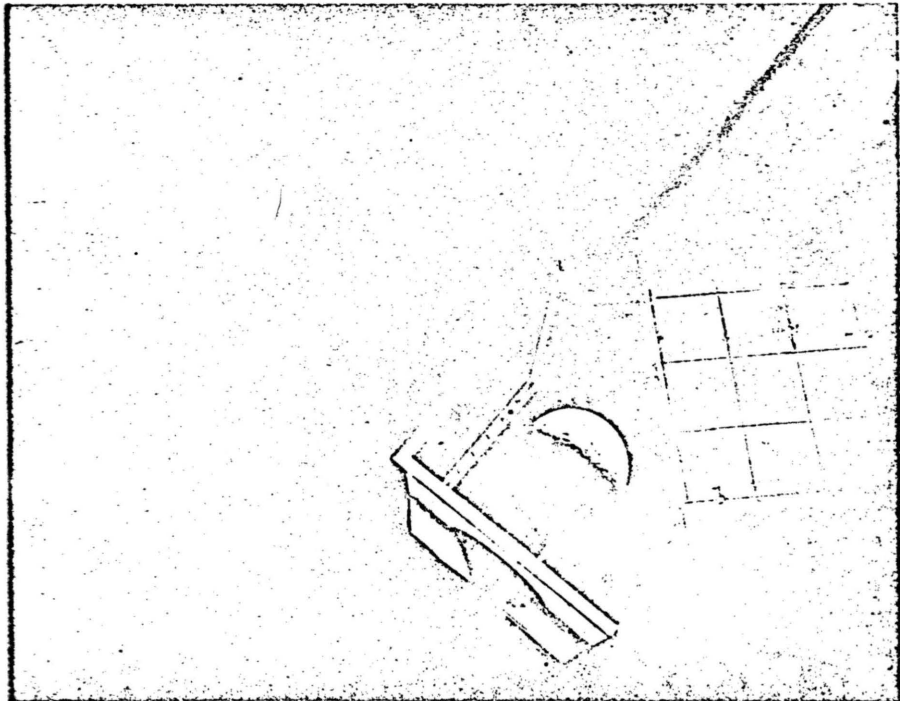
 $U_{\infty} = 5 \text{ Ft./Sec.}$ 

PHOTO 2

 $U_{\infty} = 15 \text{ Ft./Sec.}$ 

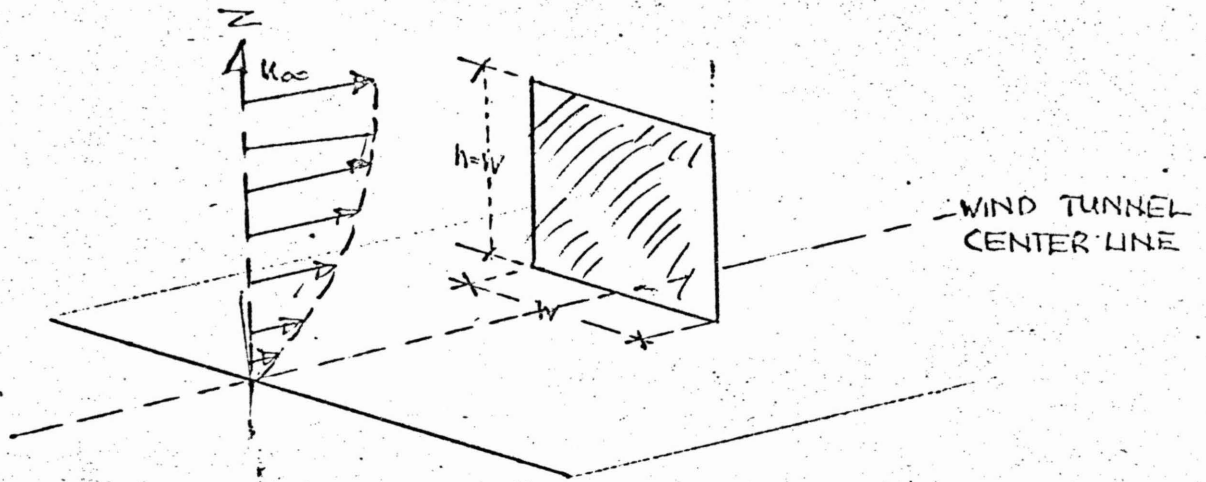


FIG 1A SCHEMATIC OF SQUARE SCREEN

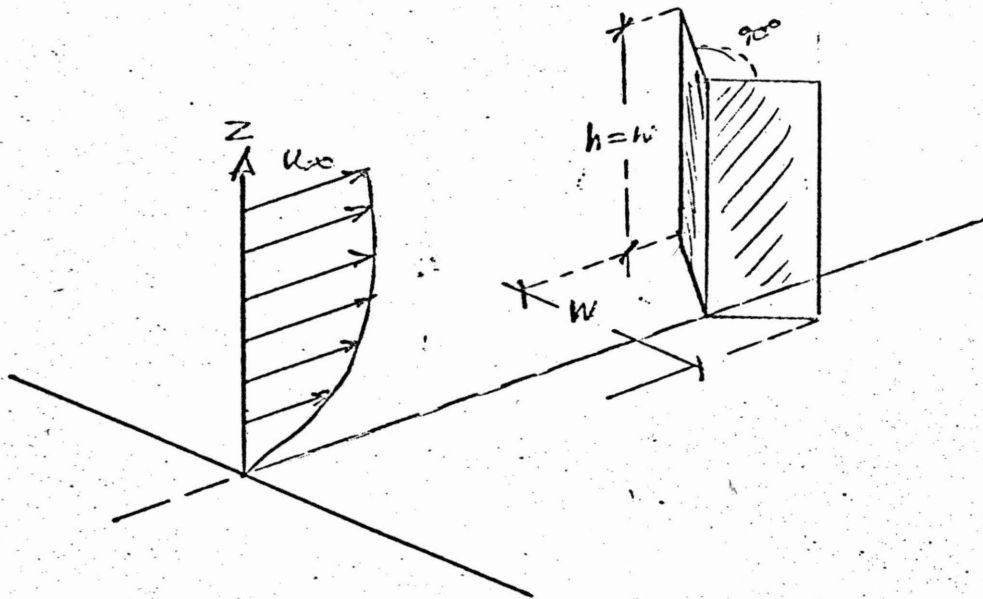


FIG 1B SCHEMATIC VIEW OF WEDGE SCREEN

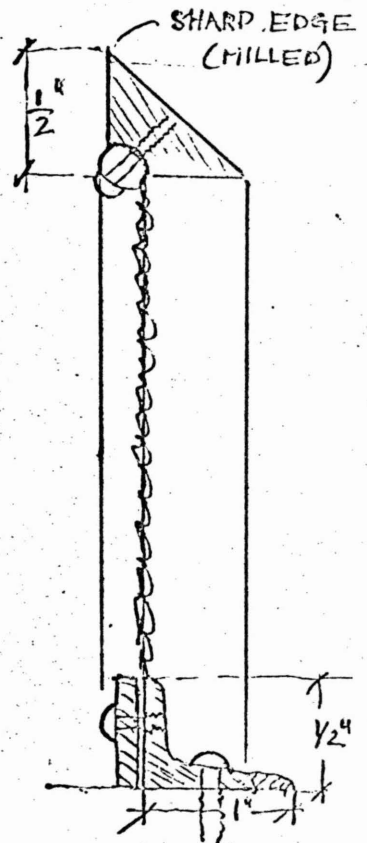
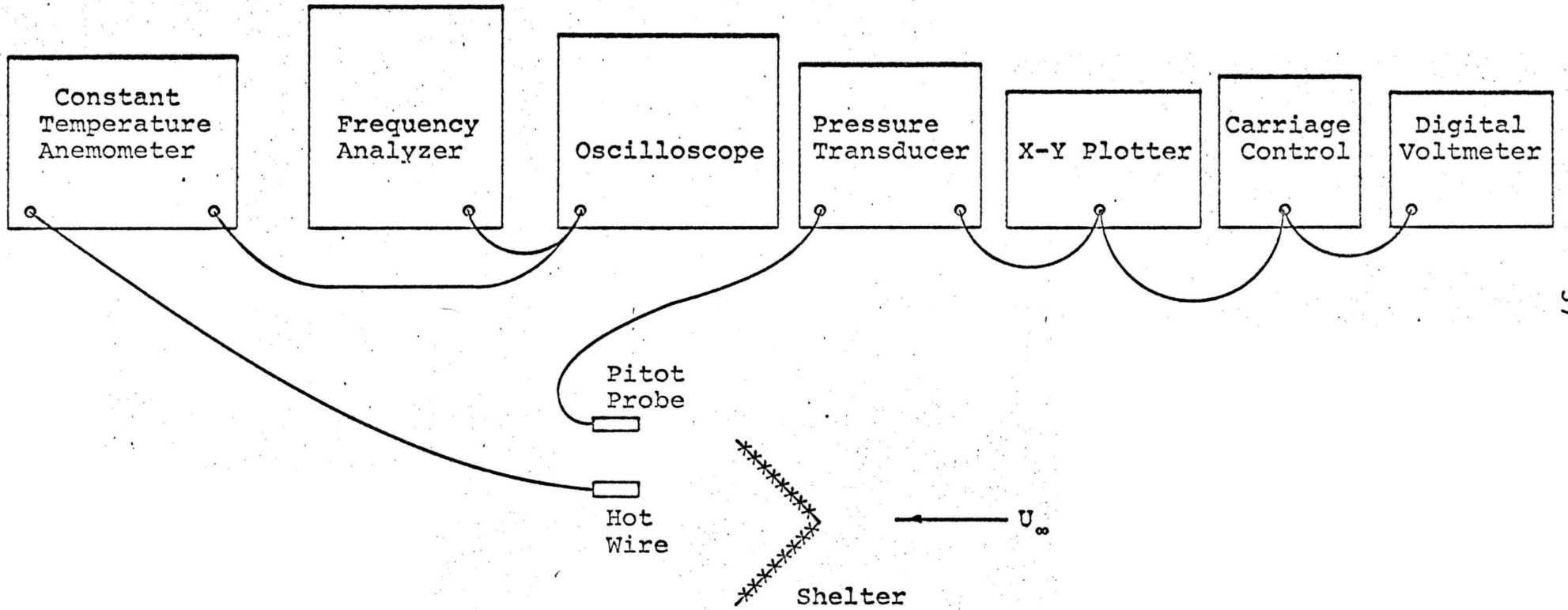


FIG 1C CONSTRUCTION DETAILS (NOT TO SCALE)

FIG 1a SCREEN MODELS

Fig. 1b Equipment lay-out



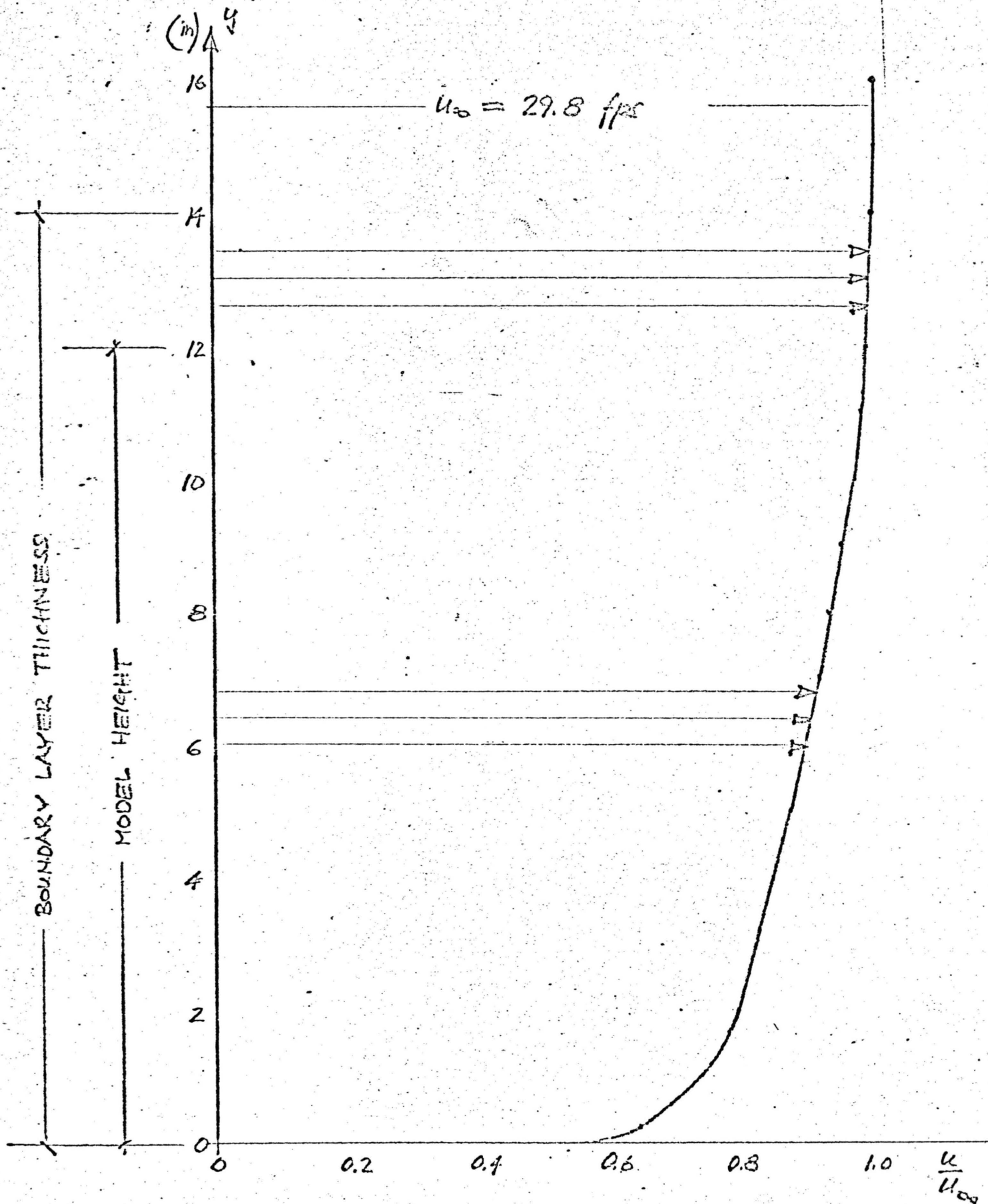
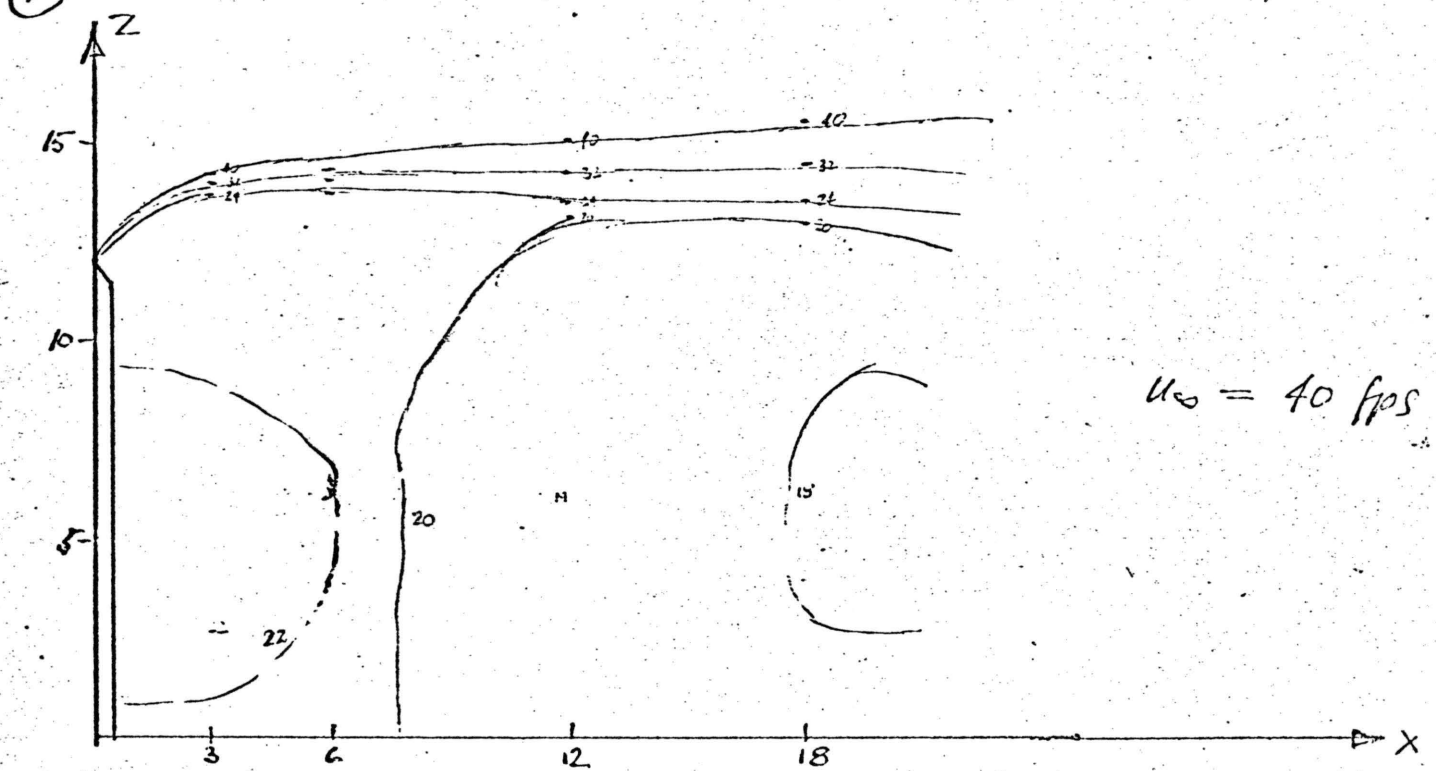
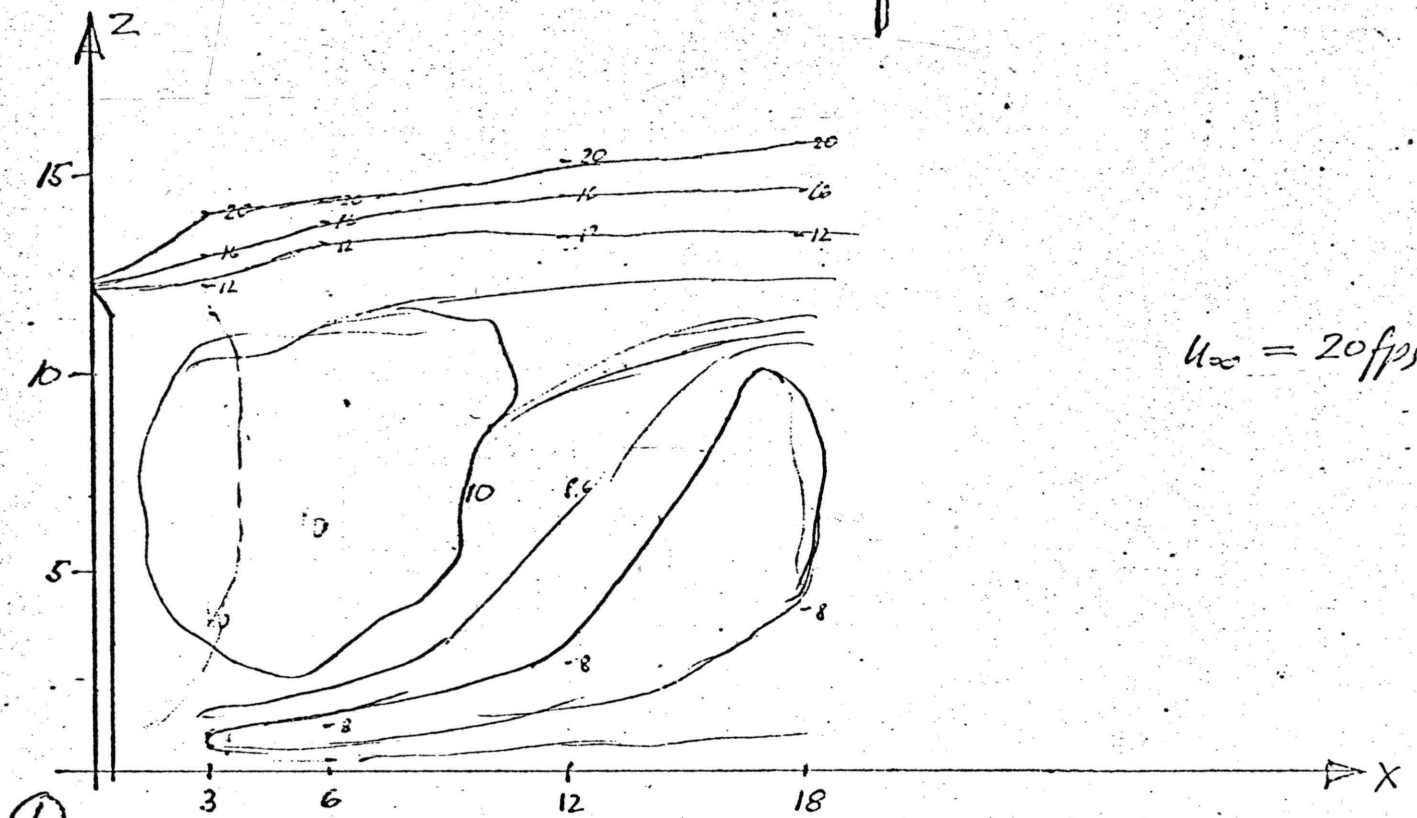
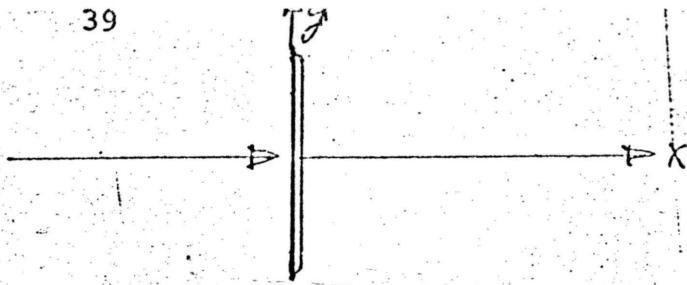


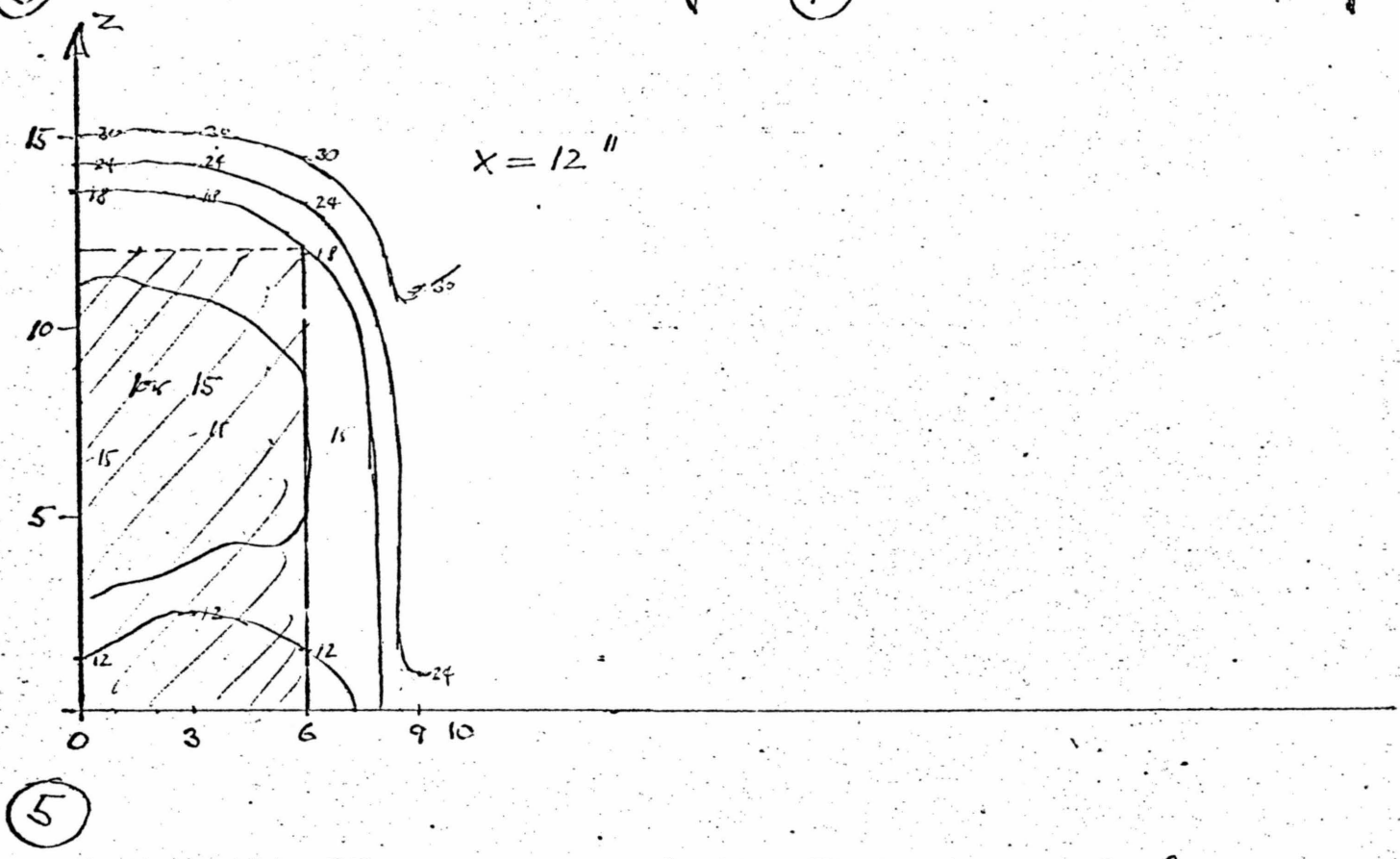
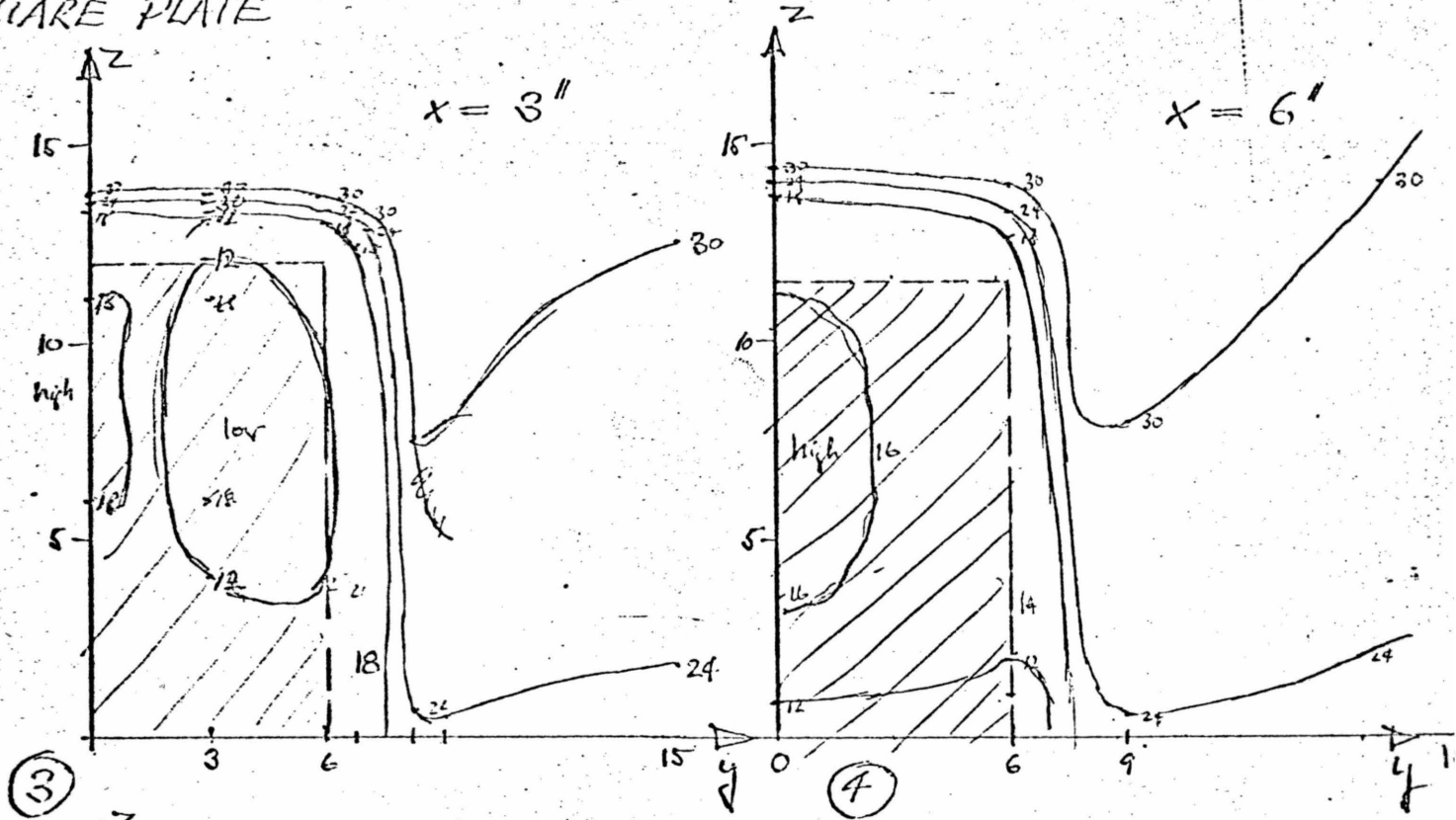
FIG 2 : APPROACH WIND PROFILE
(at $x = 5W$ upstream of model)

BUG SCREEN SQUARE PLATE



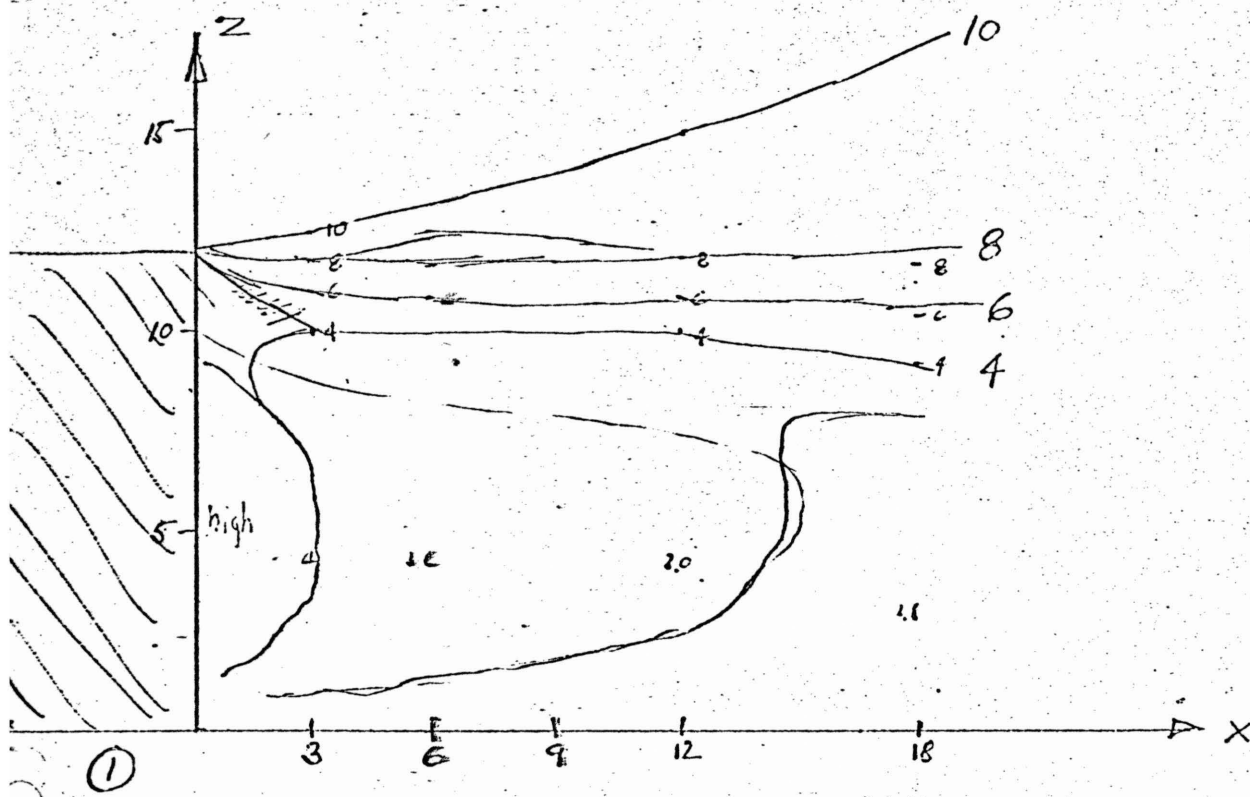
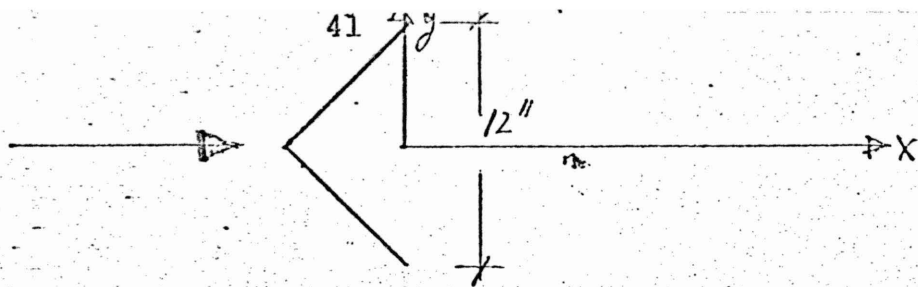
VELOCITY AT $Y=0$ (ϕ)

BUG SCREEN
SQUARE PLATE

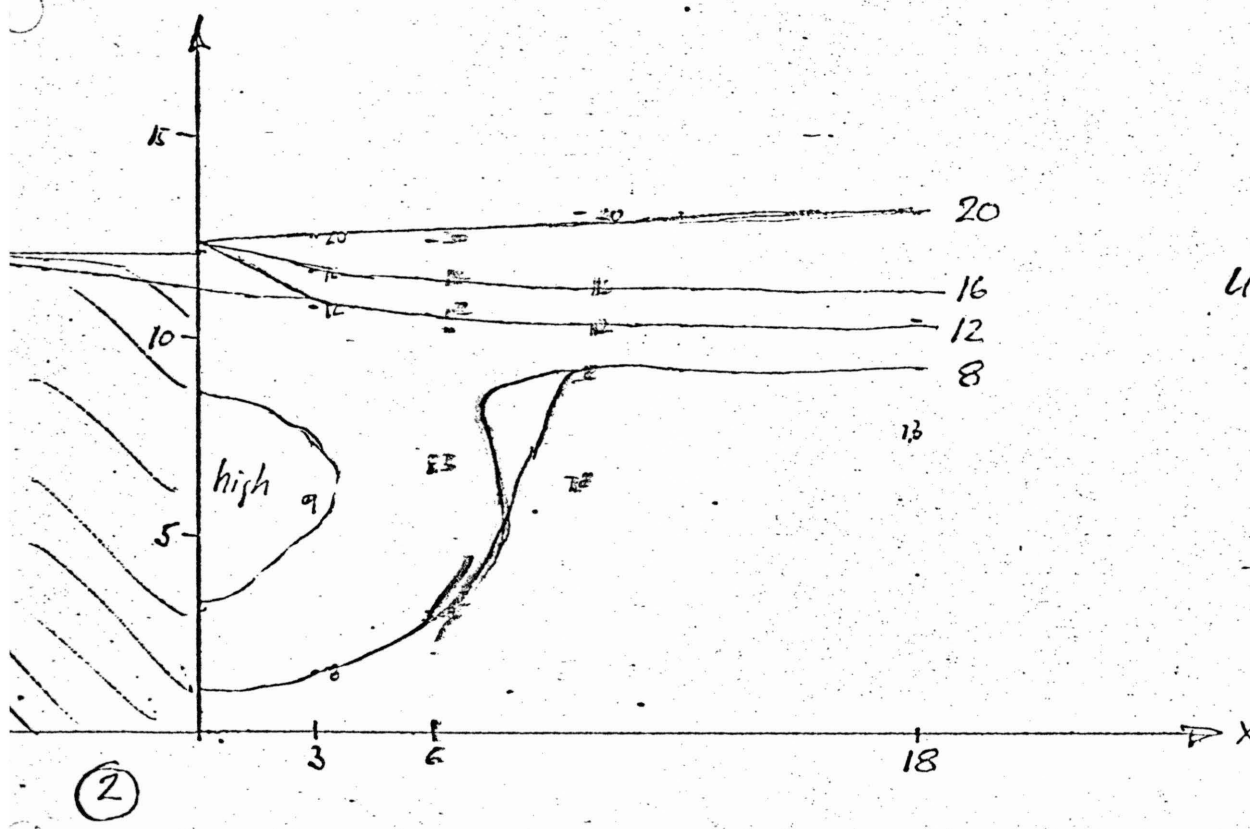


CROSS SECTIONS FOR $u_{\infty} = 30fps$

BUG SCREEN WEDGE

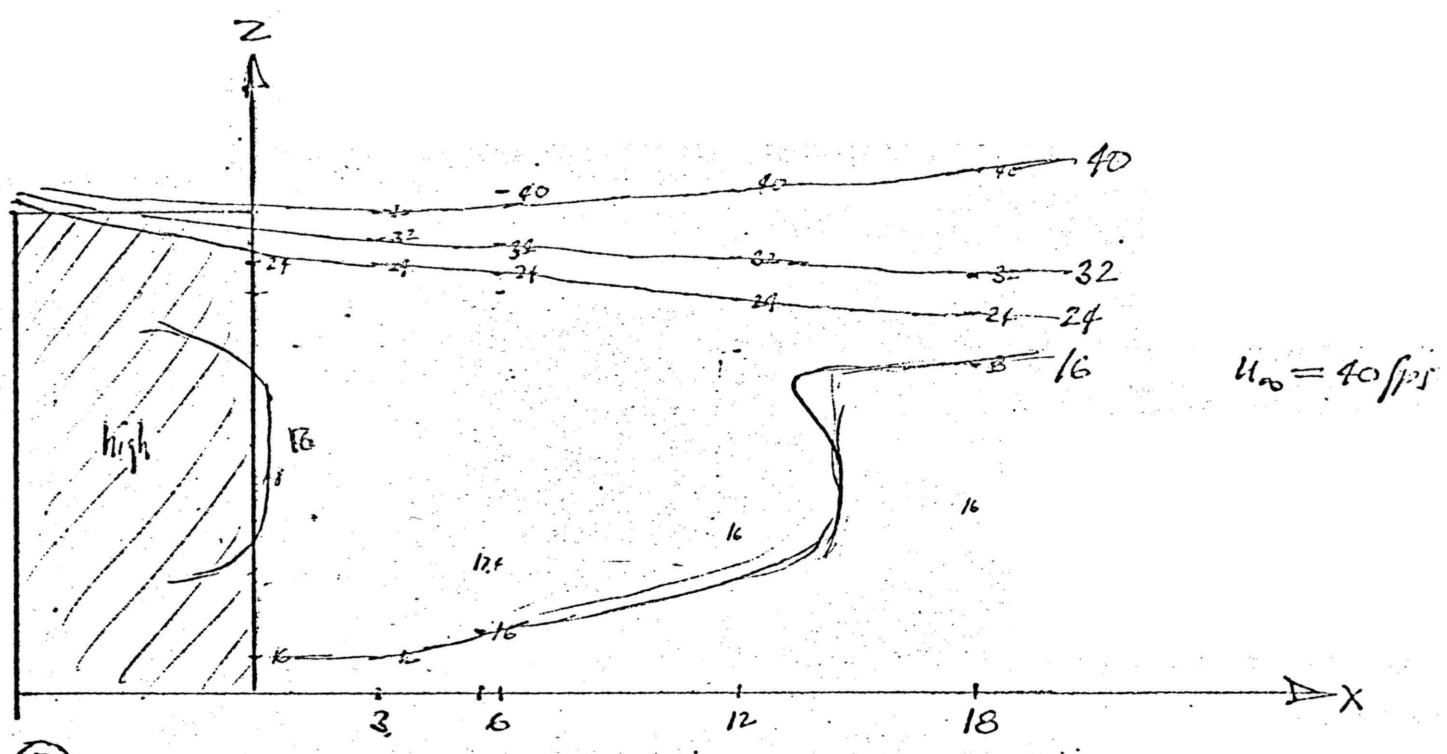


$U_{\infty} = 10 \text{ fps}$



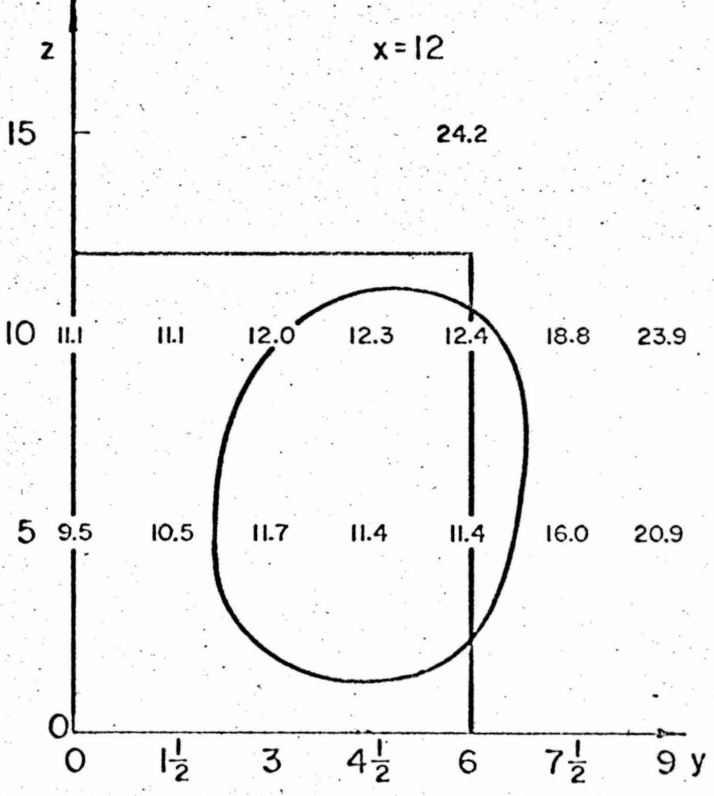
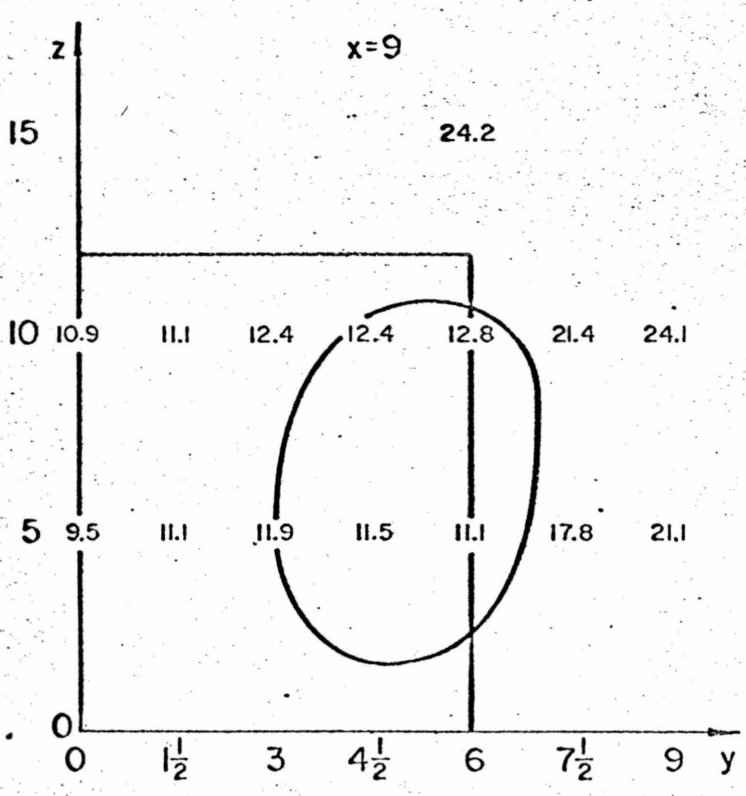
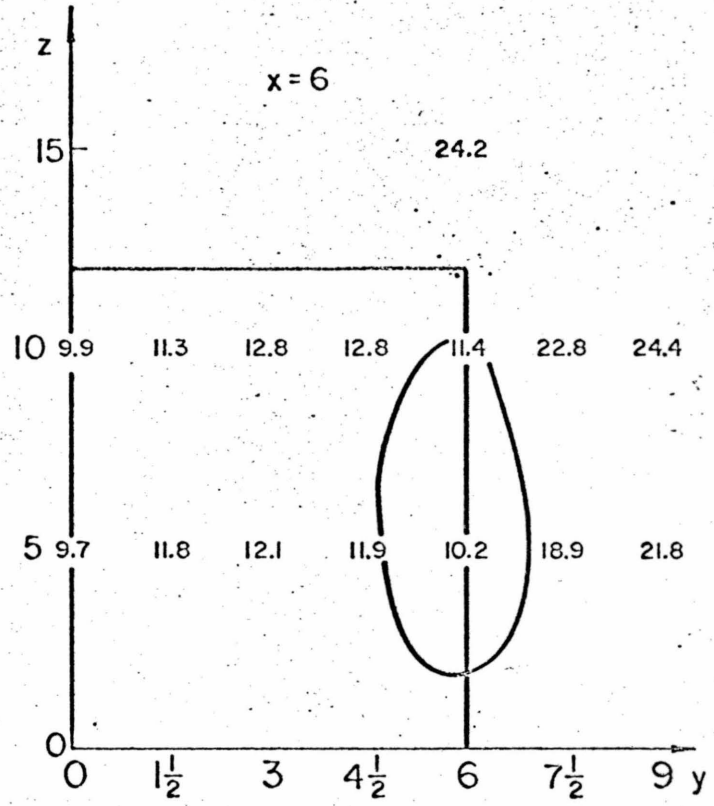
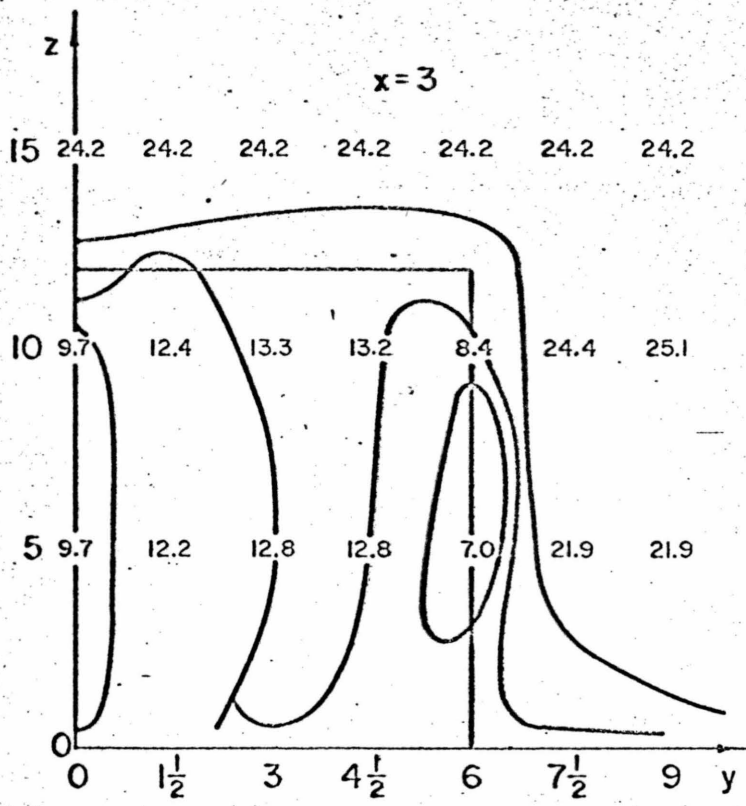
$U_{\infty} = 20 \text{ fps}$

VELOCITY AT $y=0$ (ϕ)

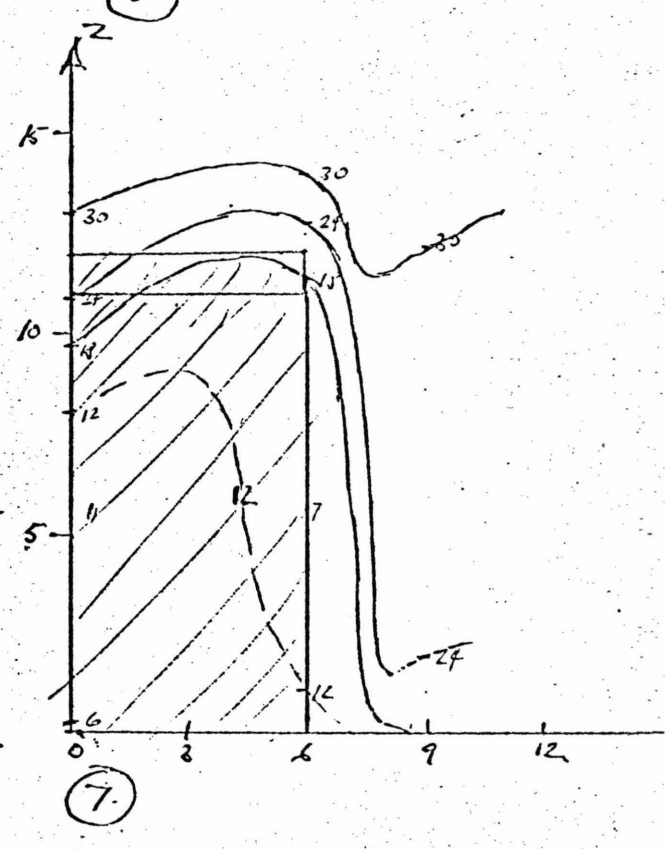
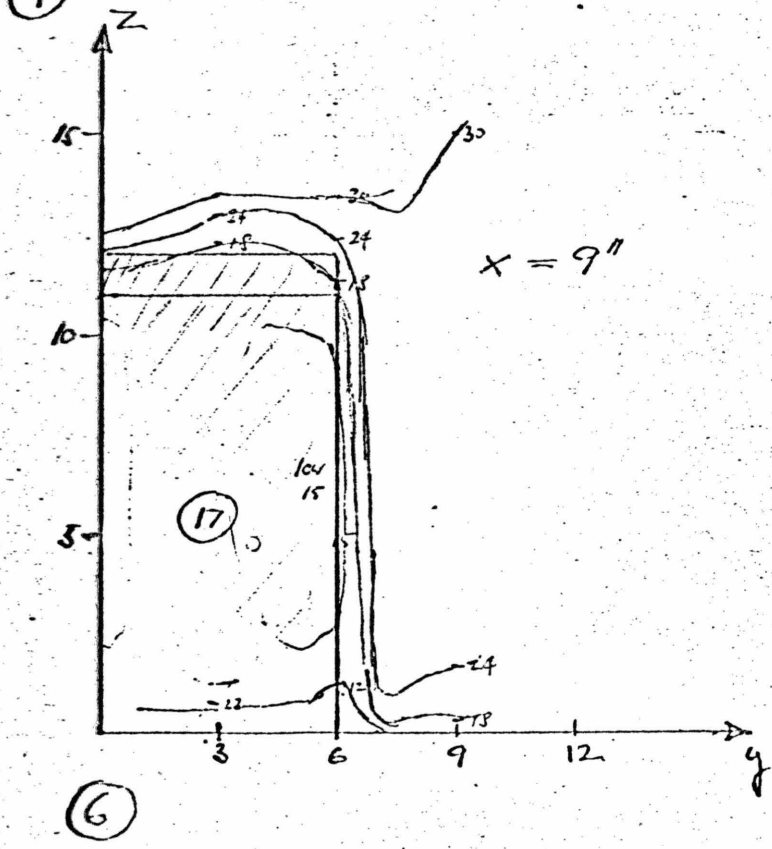
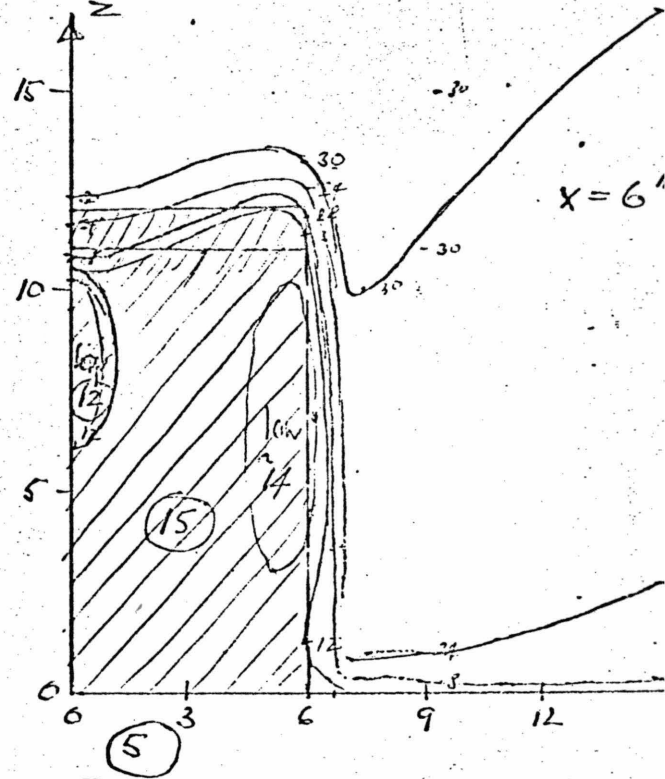
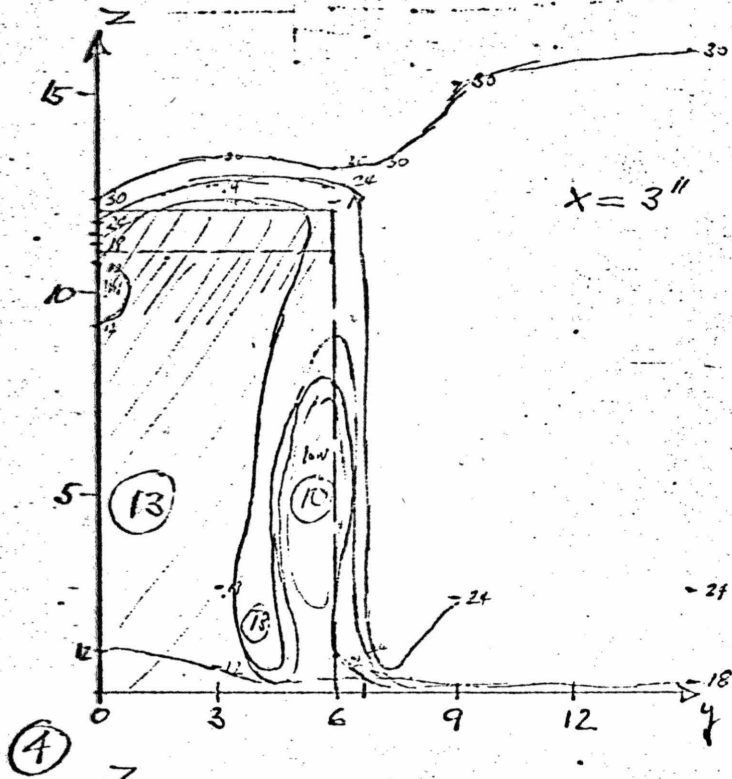


(3)

VELOCITY AT $y=0$ (ξ)

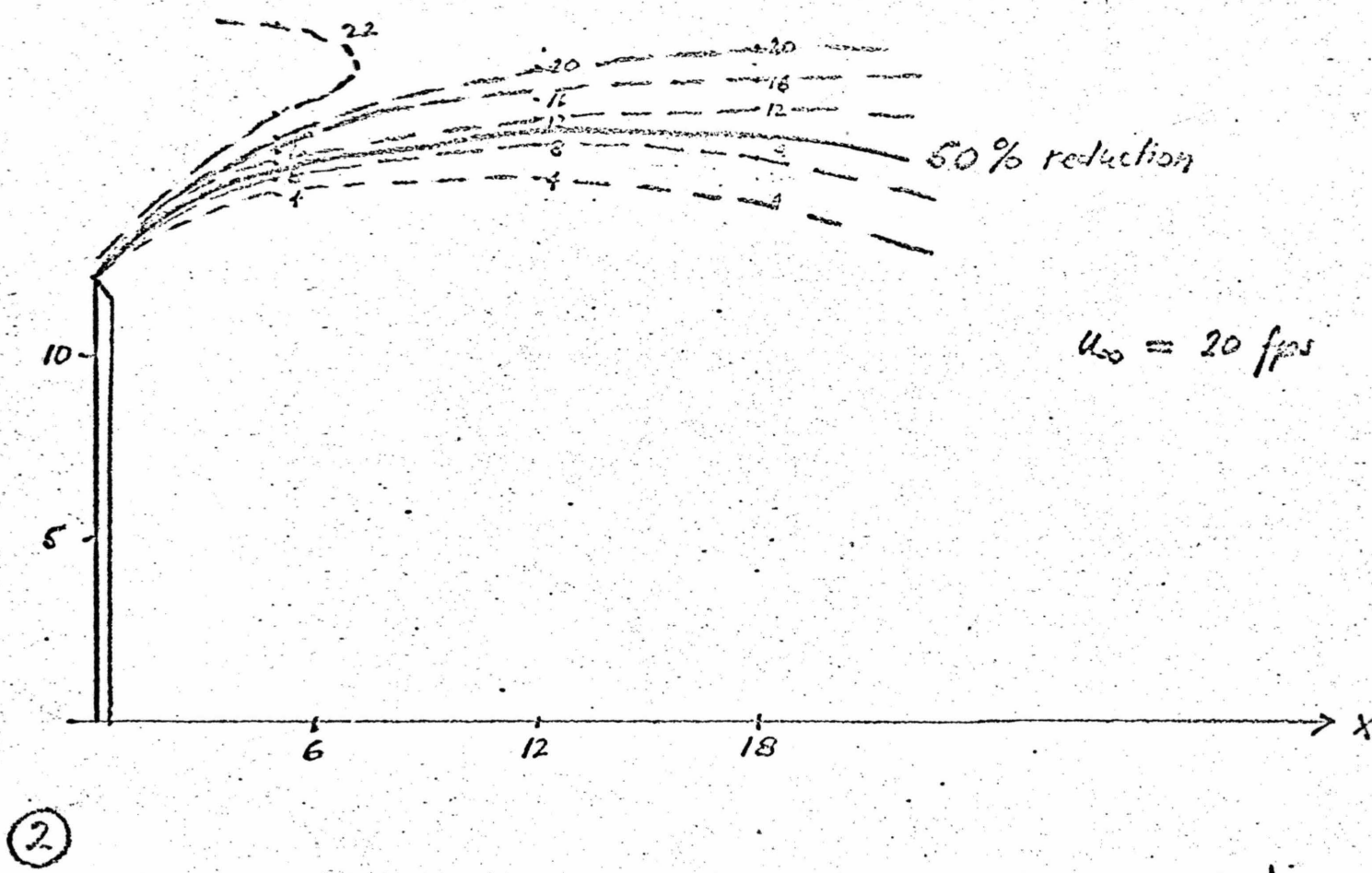
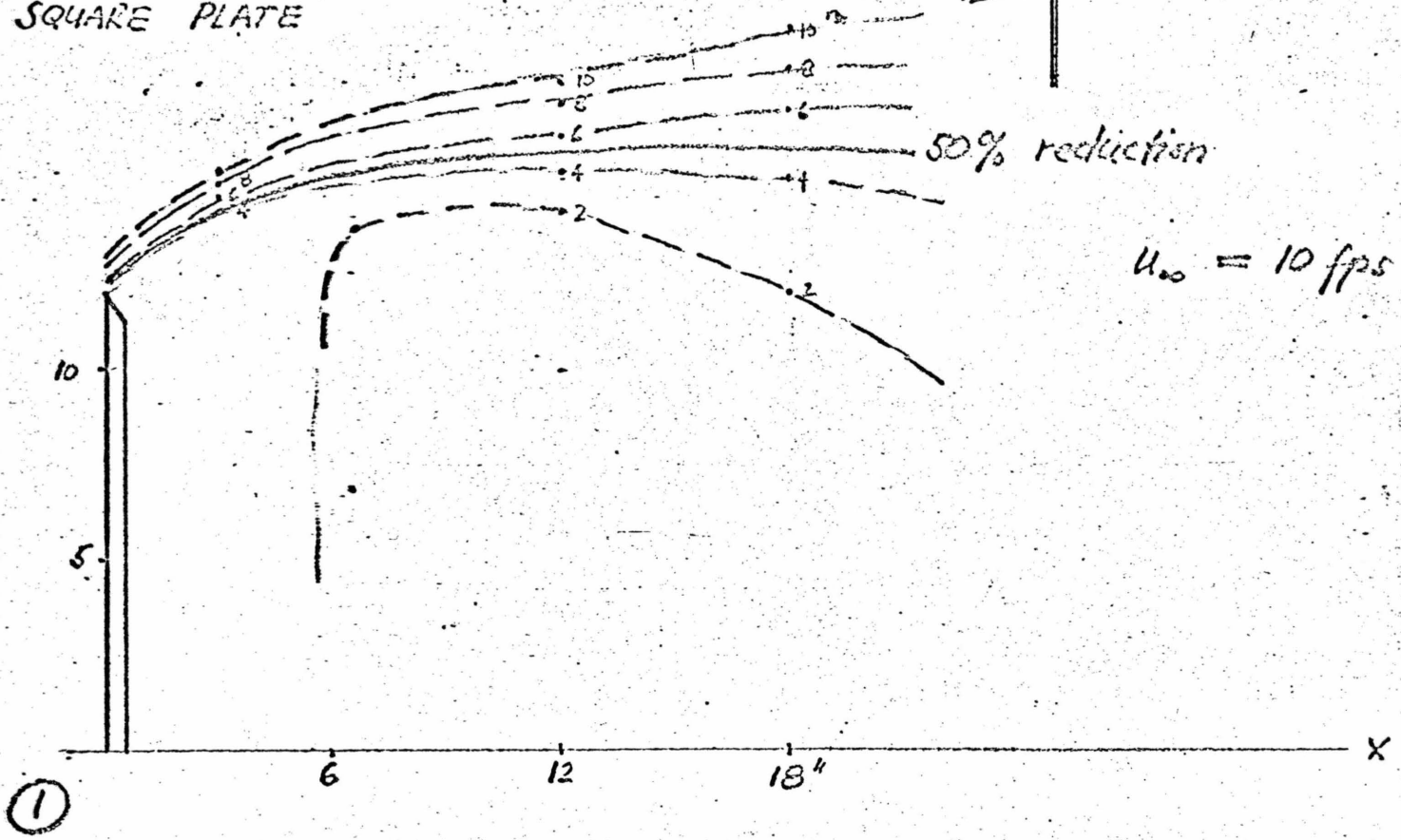


BUG SCREEN
WEDGE



CROSS SECTIONS FOR $u_{\infty} = 30$ fps
FIG. 7

NCAR - SCREEN
SQUARE PLATE



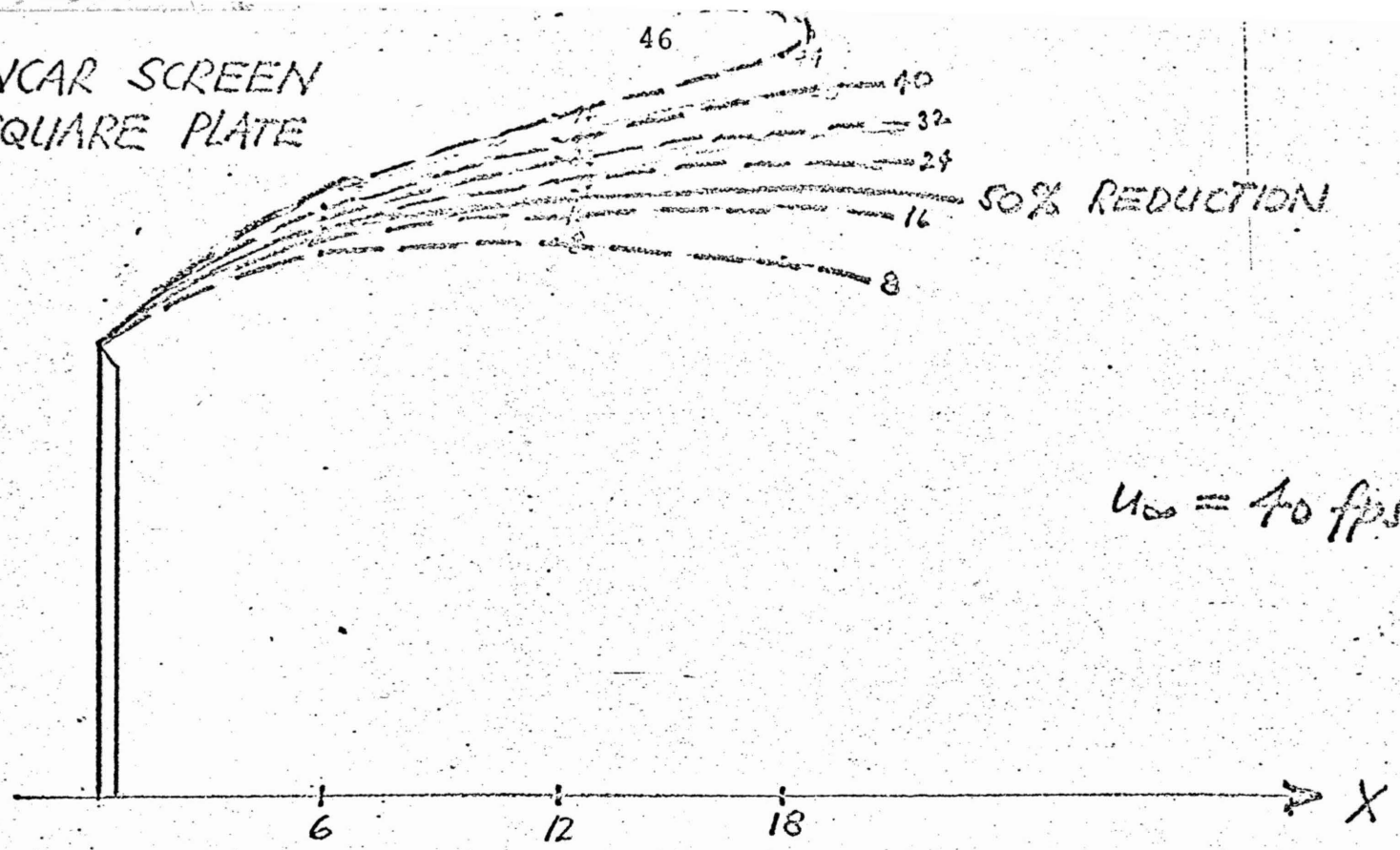
VELOCITY AT $y=0$ (ft)

NCAR SCREEN
SQUARE PLATE

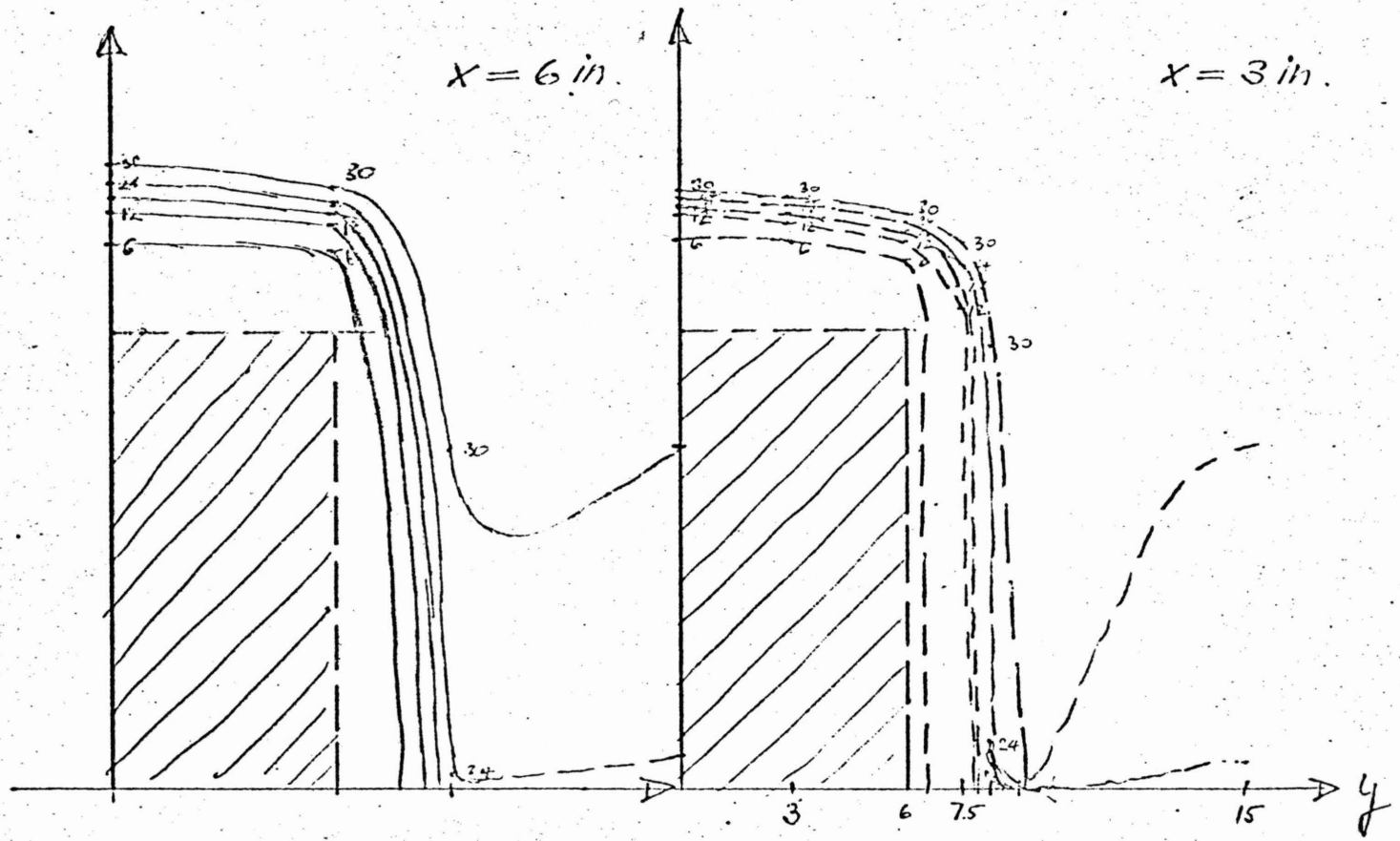
46

50% REDUCTION

$U_{\infty} = 40 \text{ fps}$



③



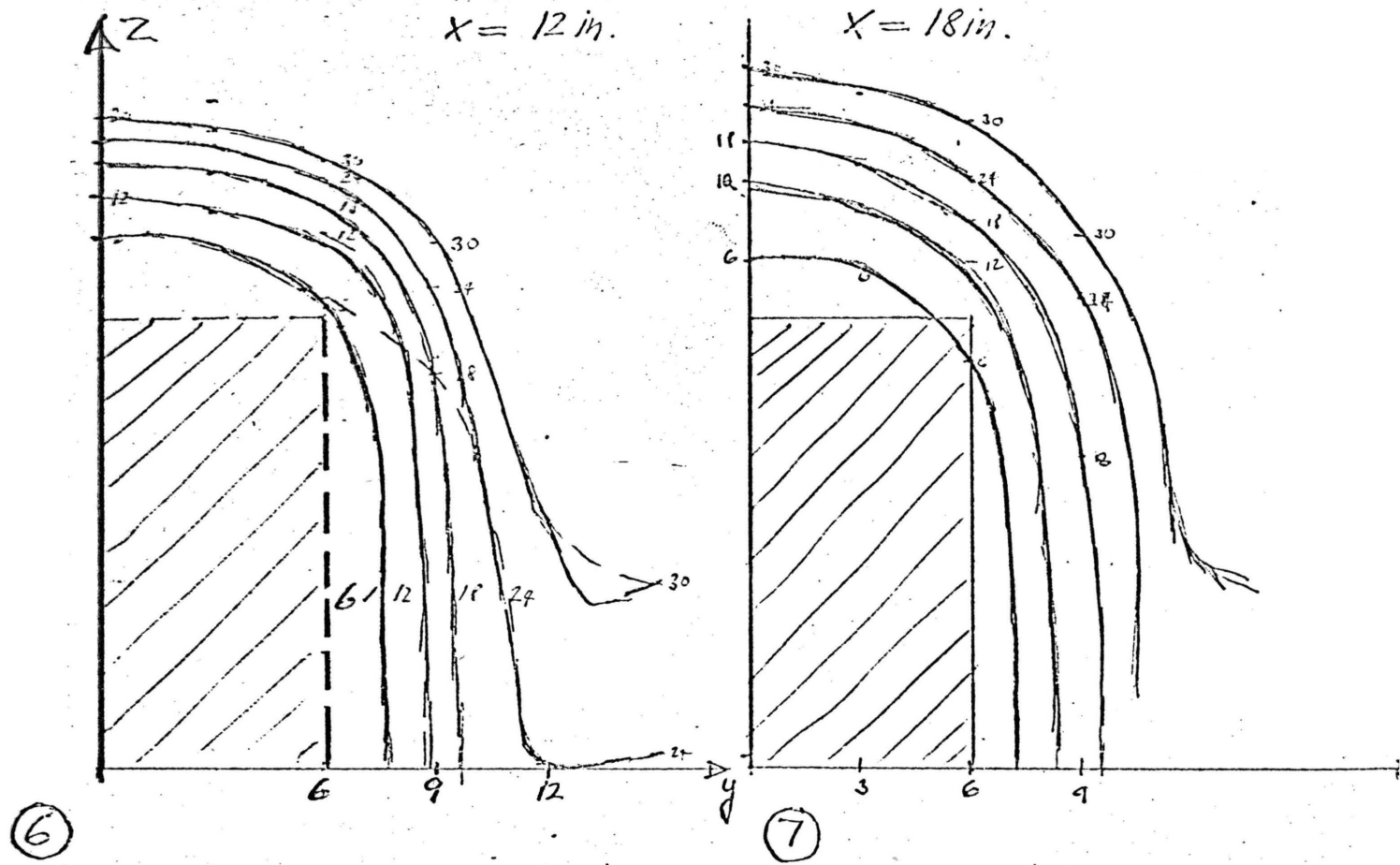
⑤

④

CROSS SECTIONS AT $U_{\infty} = 30 \text{ fps}$

Fig. 9

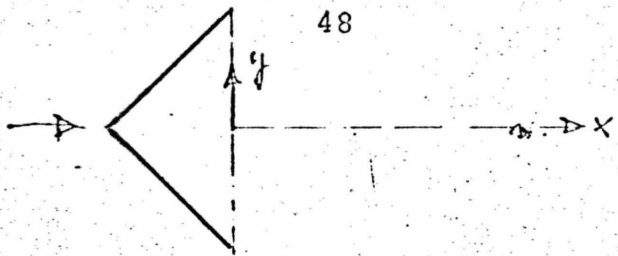
NCAR SCREEN SQUARE PLATE



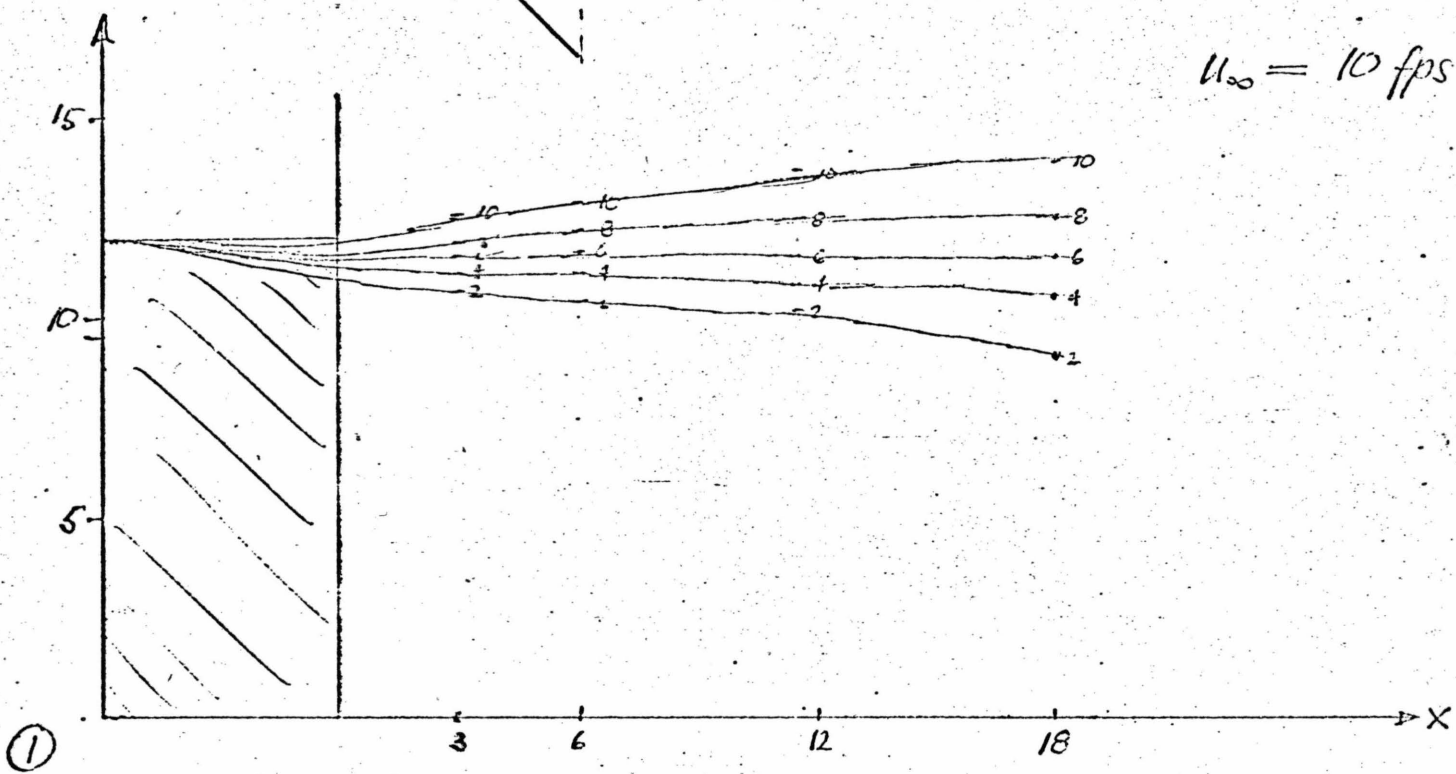
CROSS SECTIONS FOR $u_{\infty} = 30$ fps.

Fig. 10

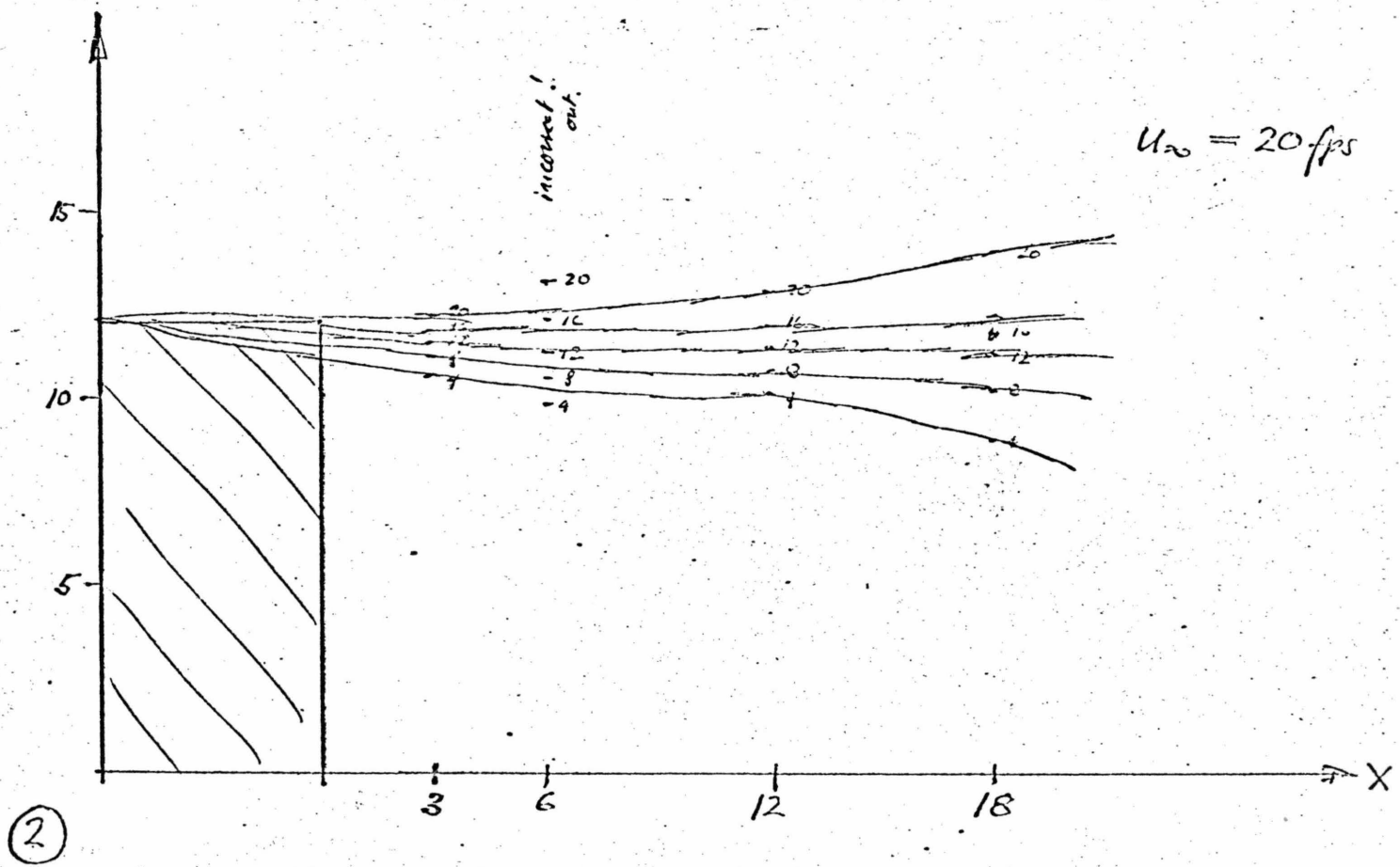
NCAR SCREEN WEDGE



$U_{\infty} = 10 \text{ fps}$



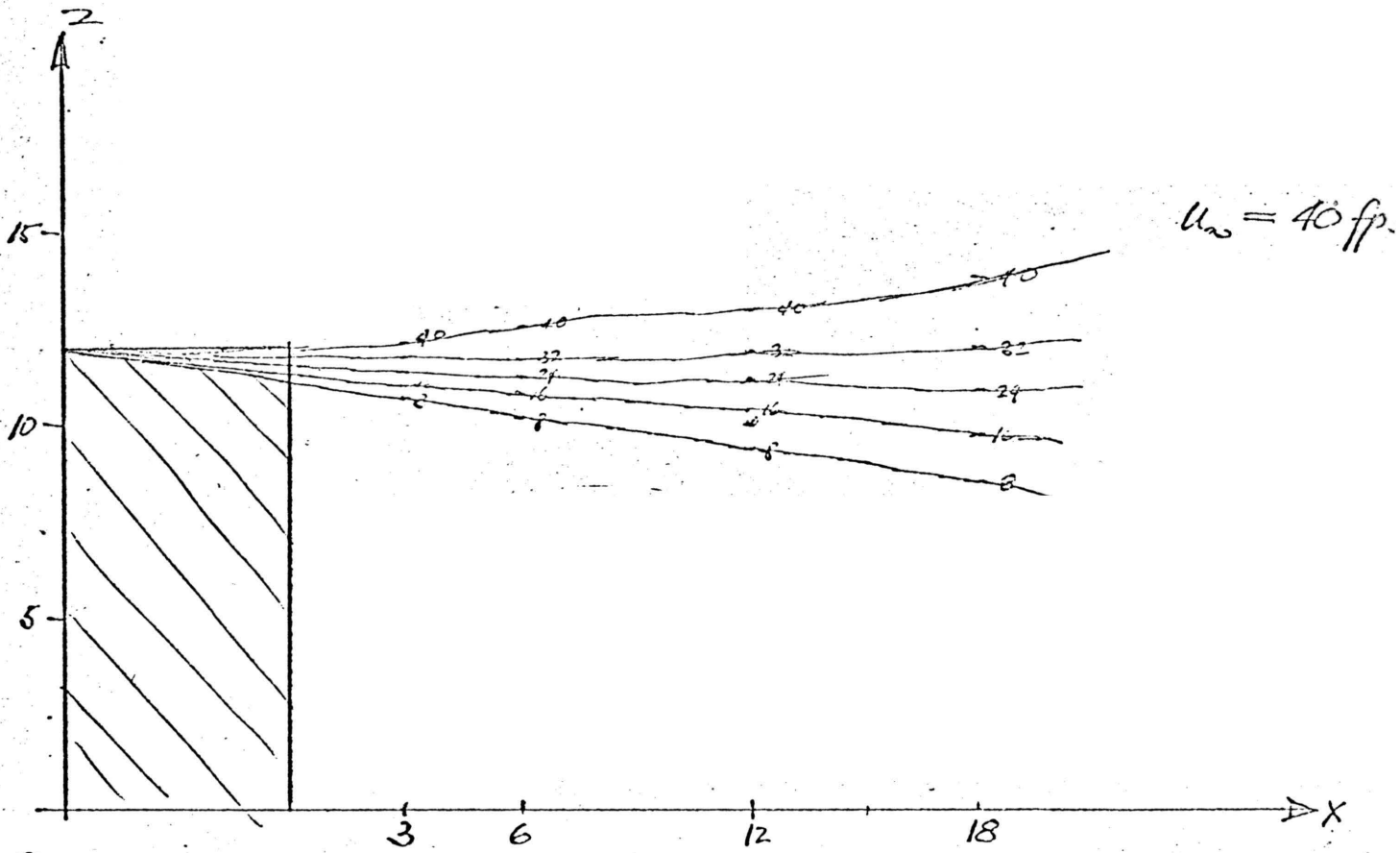
$U_{\infty} = 20 \text{ fps}$



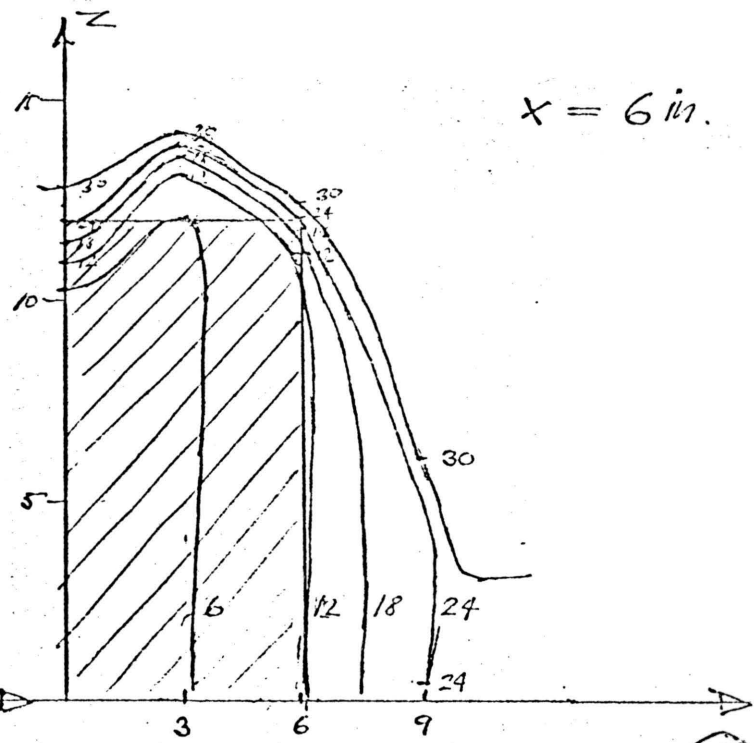
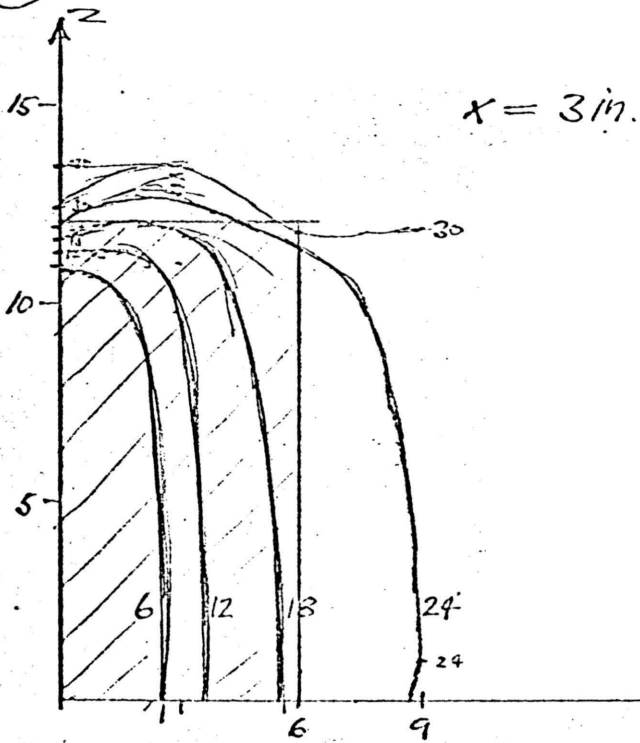
VELOCITY AT $y=0$ (ϕ)

E "

NCAR SCREEN
WEDGE



③



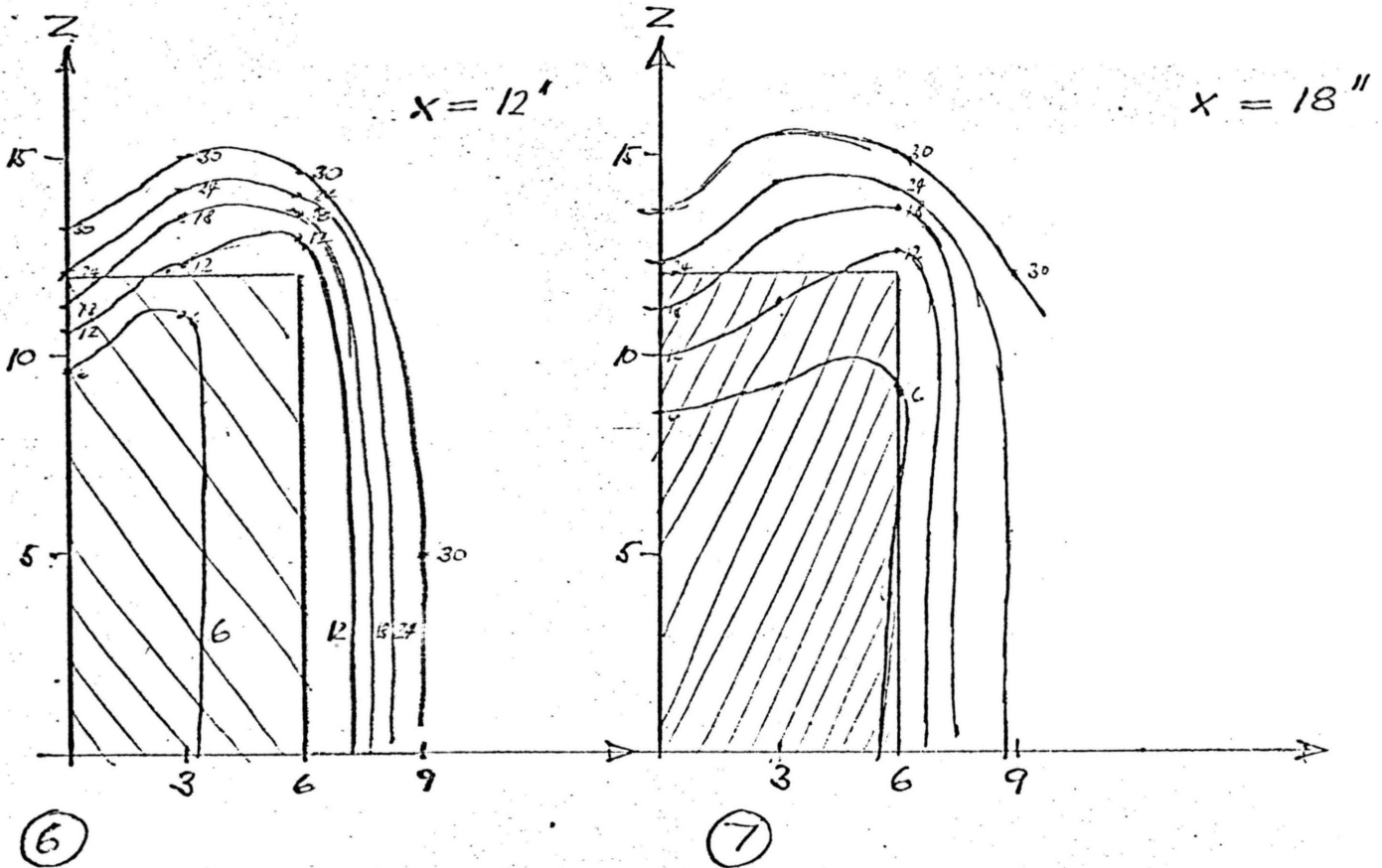
④

⑤

CROSS SECTIONS FOR $u_{\infty} = 30$ fps.

Fig. 12

NCAR SCREEN
WEDGE

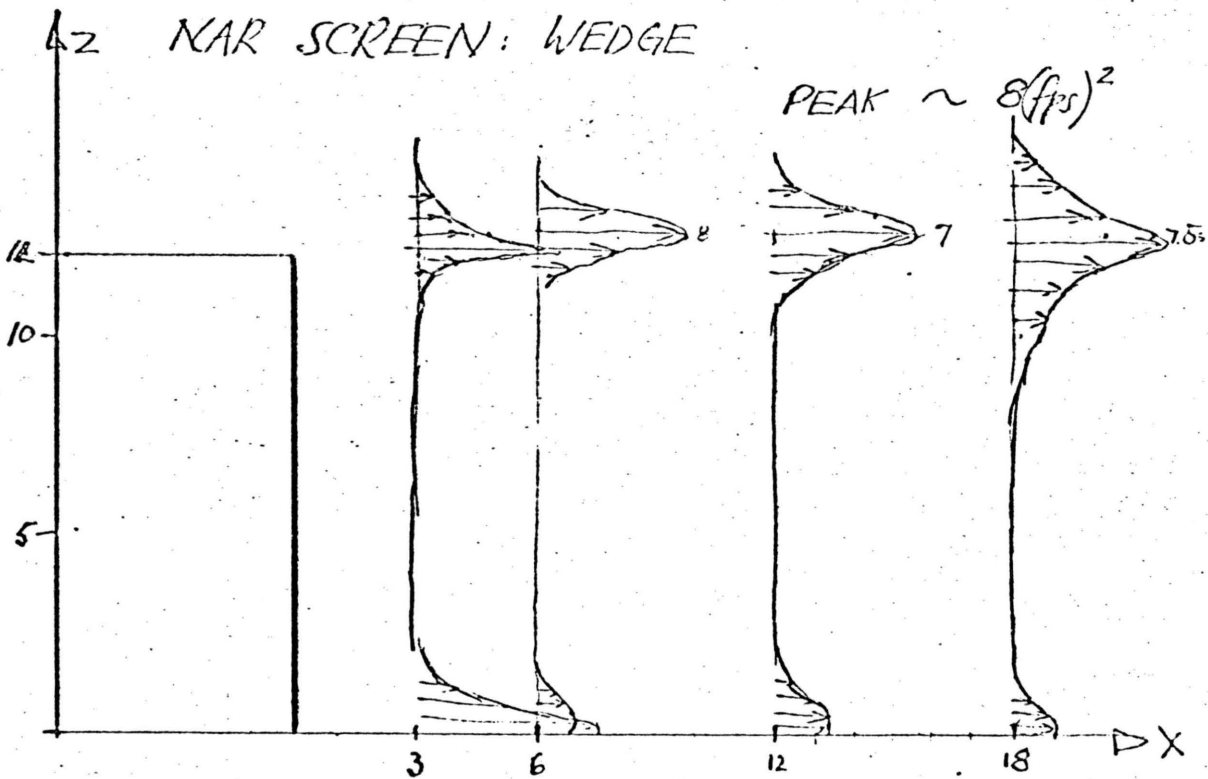
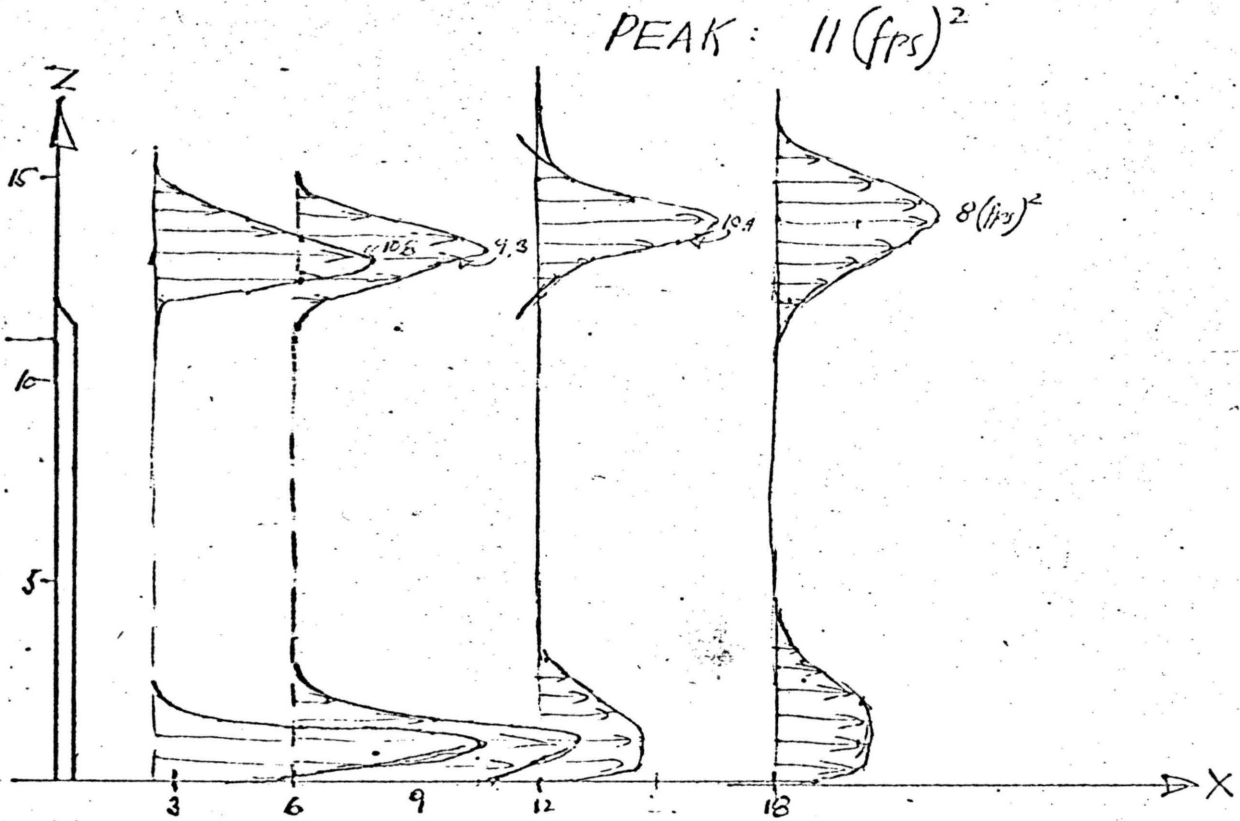


CROSS SECTIONS FOR $u_{\infty} = 30$ fps.

Fig. 13

NCAR SCREEN
SQUARE PLATE

51 PRESSURE DROP COEFF.
BIG SCREEN $\frac{\Delta P}{\frac{1}{2} \rho V^2} = 0.62$
NCAR SCREEN = 22



TURBULENT INTENSITY AT $y = \frac{1}{4} V = 3''$